using the variable pressure neck chamber. *Exp. Physiol.* 88:671–680, 2003. doi:10.1113/eph8802650.

[8]Fadel, P. J., M. Stromstad, D. W. Wray, S. A. Smith, P. B. Raven, and N. H. Secher. New insights into differential baroreflex control of heart rate in humans. *Am. J. Physiol. Heart Circ. Physiol.* 284:H735–H743, 2003.

[9]Glantz, S. A. Primer of Biostatistics. 4th ed. New York: McGraw Hill, 1997.

[10]Grassi, G., C. Turri, G. Seravalle, G. Bertinieri, A. Pierini, and G. Mancia. Effects of chronic clonidine administration on sympathetic nerve traffic and baroreflex function in heart failure. *Hypertension* 38:286–291, 2001. doi:10.1161/hy1201.096117.

[11]Grossmann, A., R. Kronland-Martinet, and J. Morlet. Reading and understanding continuous wavelets transforms. In: Wavelets, Time-Frequency Methods and Phase Space, edited by J. M. Combes, A. Grossmann, and P. Tchamitchian. Berlin: Springer, 1989, pp. 2–20.

[12]Guyton, A. C., T. G. Coleman, and H. J. Granger. Circulation: overall regulation. *Annu. Rev. Physiol.* 34:13–46, 1972. doi:10.1146/annurev.ph.34.030172.000305.

[13]Hayano, J., J. A. Taylor, S. Mukai, A. Okada, Y. Watanabe, K. Takata, and T. Fujinami. Assessment of frequency shifts in R-R interval variability and respiration with complex demodulation. *J. Appl. Physiol.* 77:2879–2888, 1994.

[14]Ichinose, M., M. Saito, N. Kondo, and T. Nishiyasu. Time-dependent modulation of arterial baroreflex control of muscle sympathetic nerve activity during isometric exercise in humans. *Am. J. Physiol. Heart Circ. Physiol.* 290:H1419–H1426, 2006. doi:10.1152/ajpheart.00847.2005.

[15]Ikeda, Y., T. Kawada, M. Sugimachi, O. Kawaguchi, T. Shishido, T. Sato, H. Miyano, W. Matsuura, J. Alexander, Jr., and K. Sunagawa. Neural arc of baroreflex optimizes dynamic pressure regulation in achieving both stability and quickness. *Am. J. Physiol. Heart Circ. Physiol.* 271:H882–H890, 1996.

[16]Jordan, J., H. R. Toka, K. Heusser, O. Toka, J. R. Shannon, J. Tank, A. Diedrich, C. Stabroth, M. Stoffels, R. Naraghi, W. Oelkers, H. Schuster, H. P. Schobel, H. Haller, and F. C. Luft. Severely impaired baroreflex-buffering in patients with monogenic hypertension and neurovascular contact. *Circulation* 102:2611–2618, 2000.

[17]Kashihara, K. Automatic regulation of hemodynamic variables in acute heart failure by a multiple adaptive predictive controller based on neural networks. *Ann. Biomed. Eng.* 34:1846–1869, 2006. doi:10.1007/s10439-006-9190-9.

[18]Kashihara, K., T. Kawada, M. Li, M. Sugimachi, and K. Sunagawa. Bezold-Jarisch reflex induced by phenylbiguanide lowers arterial pressure mainly via the downward shift of the baroreflex neural arc. *Jpn. J. Physiol.* 54:395–404, 2004. doi:10.2170/jjphysiol.54.395.

[19]Kashihara, K., T. Kawada, K. Uemura, M. Sugimachi, and K. Sunagawa. Adaptive predictive control of arterial blood pressure based on a neural network during acute hypotension. *Ann. Biomed. Eng.* 32:1365–1383, 2004. doi:10.1114/B:ABME.0000042225.19806.34.

[20]Kashihara, K., T. Kawada, Y. Yanagiya, K. Uemura, M. Inagaki, H. Takaki, M. Sugimachi, and K. Sunagawa. Bezold-Jarisch reflex attenuates dynamic gain of baroreflex neural arc. *Am. J. Physiol. Heart Circ. Physiol.* 285:H833–H840, 2003.

[21]Kashihara, K., Y. Takahashi, K. Chatani, T. Kawada, C. Zheng, M. Li, M. Sugimachi, and K. Sunagawa. Intravenous angiotensin II does not affect dynamic baroreflex characteristics of the neural or peripheral arc. *Jpn. J. Physiol.* 53:135–143, 2003. doi:10.2170/jjphysiol.53.135.

[22]Kawada, T., T. Miyamoto, K. Uemura, K. Kashihara, A. Kamiya, M. Sugimachi, and K. Sunagawa. Effects of neuronal norepinephrine uptake blockade on baroreflex neural and peripheral arc transfer characteristics. *Am. J. Physiol. Regul. Integr. Comp. Physiol.* 286:R1110–1120, 2004. doi:10.1152/ajpregu.00527.2003.

[23]Kawada, T., Y. Yanagiya, K. Uemura, T. Miyamoto, C. Zheng, M. Li, M. Sugimachi, and K. Sunagawa. Input-size dependence of the baroreflex neural arc transfer characteristics. *Am. J. Physiol. Heart Circ. Physiol.* 284:H404–H415, 2003.

[24]Kent, B. B., J. W. Drane, B. Blumenstein, and J. W. Manning. A mathematical model to assess changes in the baroreceptor reflex. *Cardiology* 57:295–310, 1972.

[25]Landesberg, G., D. Adam, Y. Berlatzky, and S. Akselrod. Step baroreflex response in awake patients undergoing carotid surgery: time- and frequency-domain analysis. *Am. J. Physiol.* 274:H1590–H1597, 1998.

[26]Lee, D. Coherent oscillations in neuronal activity of the supplementary motor area during a visuomotor task. *J. Neurosci.* 23:6798–6809, 2003.

[27]Lipman, R. D., J. K. Salisbury, and J. A. Taylor. Spontaneous indices are inconsistent with arterial baroreflex gain. *Hypertension* 42:481–487, 2003. doi:10.1161/01.HYP.0000091370.83602.E6.

[28]Liu, H. K., S. J. Guild, J. V. Ringwood, C. J. Barrett, B. L. Leonard, S. K. Nguang, M. A. Navakatikyan, and S. C. Malpas. Dynamic baroreflex control of blood pressure: influence of the heart vs. peripheral resistance. *Am. J. Physiol. Regul. Integr. Comp. Physiol.* 283:R533–R542, 2002.

[29]Lucini, D., M. Pagani, G. S. Mela, and A. Malliani. Sympathetic restraint of baroreflex control of heart period in normotensive and hypertensive subjects. *Clin. Sci. (Lond.)* 86:547–556, 1994.

[30]Malliani, A., M. Pagani, F. Lombardi, and S. Cerutti. Cardiovascular neural regulation explored in the frequency domain. *Circulation* 84:482–492, 1991.

[31]Marmarelis, P. Z., and V. Z. Marmarelis. The white noise method in system identification. In: Analysis of Physiological Systems. New York: Plenum, 1978, pp. 131–221.

[32]Masaki, H., T. Imaizumi, Y. Harasawa, and A. Takeshita. Dynamic arterial baroreflex in rabbits with heart failure induced by rapid pacing. *Am. J. Physiol.* 267:H92–H99, 1994.

[33]Mohrman, D. E., and L. J. Heller. Cardiovascular Physiology. 4th ed. New York: McGraw-Hill, 1997.

[34]Motard, R. L., and B. Joseph. Wavelet Applications in Chemical Engineering. Boston: Kluwer Academic Publishers, 1994.

[35]Munakata, M., Y. Imai, H. Takagi, M. Nakao, M. Yamamoto, and K. Abe. Altered frequency-dependent characteristics of the cardiac baroreflex in essential hypertension. *J. Auton. Nerv. Syst.* 49:33–45, 1994. doi:10.1016/0165-1838(94)90018-3.

[36]Osculati, G., G. Grassi, C. Giannattasio, G. Seravalle, F. Valagussa, A. Zanchetti, and G. Mancia. Early alterations of the baroreceptor control of heart rate in patients with acute myocardial infarction. *Circulation* 81:939–948, 1990.

[37]Parati, G., M. DiRienzo, and G. Mancia. Dynamic modulation of baroreflex sensitivity in health and disease. *Ann. NY Acad. Sci.* 940:469–487, 2001.

[38]Parati, G., J. P. Saul, and P. Castiglioni. Assessing arterial baroreflex control of heart rate: new perspectives. *J. Hypertens.* 22:1259–1263, 2004. doi:10.1097/01.hjh.0000125469.35523.32.

[39]Parmer, R. J., J. H. Cervenka, and R. A. Stone. Baroreflex sensitivity and heredity in essential hypertension. *Circulation* 85:497–503, 1992.

[40]Persson, P. B., M. DiRienzo, P. Castiglioni, C. Cerutti, M. Pagani, N. Honzikova, S. Akselrod, and G. Parati. Time versus frequency domain techniques for assessing baroreflex sensitivity. *J. Hypertens.* 19:1699–1705, 2001. doi:10.1097/00004872-200110000-00001.

[41]Pinna, G. D., R. Maestri, G. Raczak, and M. T. La Rovere. Measuring baroreflex sensitivity from the gain function between arterial pressure and heart period. *Clin. Sci. (Lond.)* 103:81–88, 2002.

[42]Pitzalis, M. V., F. Mastropasqua, A. Passantino, F. Massari, L. Ligurgo, C. Forleo, C. Balducci, F. Lombardi, and P. Rizzon. Comparison between noninvasive indices of baroreceptor sensitivity and the phenylephrine method in post-myocardial infarction patients. *Circulation* 97:1362–1367, 1998.

[43]Porta, A., G. Baselli, O. Rimoldi, A. Malliani, and M. Pagani. Assessing baroreflex gain from spontaneous variability in conscious dogs: role of causality and respiration. *Am. J. Physiol. Heart Circ. Physiol.* 279:H2558–H2567, 2000.

[44]Radaelli, A., L. Bernardi, F. Valle, S. Leuzzi, F. Salvucci, L. Pedrotti, E. Marchesi, G. Finardi, and P. Sleight. Cardiovascular autonomic modulation in essential hypertension. Effect of tilting. *Hypertension* 24:556–563, 1994.

[45]Rudas, L., A. A. Crossman, C. A. Morillo, J. R. Halliwill, K. U. Tahvanainen, T. A. Kuusela, and D. L. Eckberg. Human sympathetic and vagal baroreflex responses to sequential nitroprusside and phenylephrine. *Am. J. Physiol.* 276:H1691–H1698, 1999.

[46]Sagawa, K. Baroreflex control of systemic arterial pressure and vascular bed. In: Handbook of Physiology. The Cardiovascular System. Peripheral Circulation and Organ Blood Flow, sect. 2, vol. III, pt. 2, chap. 14. Bethesda, MD: Am. Physiol. Soc., 1983, pp. 453–496.

[47]Sato, T., T. Kawada, M. Inagaki, T. Shishido, H. Takaki, M. Sugimachi, and K. Sunagawa. New analytic framework for understanding sympathetic baroreflex control of arterial pressure. *Am. J. Physiol.* 276:H2251–H2261, 1999.

[48]Sinkkonen, J., H. Tiitinen, and R. Naatanen. Gabor filters: an informative way for analysing event-related brain activity. *J. Neurosci. Methods* 56:99–104, 1995. doi:10.1016/0165-0270(94)00111-S.

[49]Tallon-Baudry, C., O. Bertrand, C. Delpuech, and J. Pernier. Stimulus specificity of phase-locked and non-phase-locked 40 Hz visual responses in human. *J. Neurosci.* 16:4240–4249, 1996.

[50]Toledo, E., O. Gurevitz, H. Hod, M. Eldar, and S. Akselrod. Wavelet analysis of instantaneous heart rate: a study of autonomic control during thrombolysis. *Am. J. Physiol. Regul. Integr. Comp. Physiol.* 284:R1079–R1091, 2003.

[51]Westerhof, B. E., J. Gisolf, J. M. Karemaker, K. H. Wesseling, N. H. Secher, and J. J. van Lieshout. Time course analysis of baroreflex sensitivity during postural stress. *Am. J. Physiol. Heart Circ. Physiol.* 291:H2864–H2874, 2006. doi:10.1152/ajpheart.01024.2005.

[52]Zhang, R., K. Behbehani, C. G. Crandall, J. H. Zuckerman, and B. D. Levine. Dynamic regulation of heart rate during acute hypotension: new insight into baroreflex function. *Am. J. Physiol. Heart Circ. Physiol.* 280:H407–H419, 2001.

Am J Physiol Heart Circ Physiol 296: H1666–H1674, 2009.
First published February 27, 2009; doi:10.1152/ajpheart.01041.2008.

Angiotensin II disproportionally attenuates dynamic vagal and sympathetic heart rate controls

Toru Kawada,[1] Masaki Mizuno,[1] Shuji Shimizu,[2] Kazunori Uemura,[1] Atsunori Kamiya,[1] and Masaru Sugimachi[1]

[1]*Department of Cardiovascular Dynamics, Advanced Medical Engineering Center, National Cardiovascular Center Research Institute, Osaka and* [2]*Japan Association for the Advancement of Medical Equipment, Tokyo, Japan*

Submitted 29 September 2008; accepted in final form 25 February 2009

Kawada T, Mizuno M, Shimizu S, Uemura K, Kamiya A, Sugimachi M. Angiotensin II disproportionally attenuates dynamic vagal and sympathetic heart rate controls. *Am J Physiol Heart Circ Physiol* 296: H1666–H1674, 2009. First published February 27, 2009; doi:10.1152/ajpheart.01041.2008.—To better understand the pathophysiological role of angiotensin II (ANG II) in the dynamic autonomic regulation of heart rate (HR), we examined the effects of intravenous administration of ANG II (10 $\mu g \cdot kg^{-1} \cdot h^{-1}$) on the transfer function from vagal or sympathetic nerve stimulation to HR in anesthetized rabbits with sinoaortic denervation and vagotomy. In the vagal stimulation group (n = 7), we stimulated the right vagal nerve for 10 min using binary white noise (0–10 Hz). The transfer function from vagal stimulation to HR approximated a first-order low-pass filter with pure delay. ANG II attenuated the dynamic gain from 7.6 ± 0.9 to 5.8 ± 0.9 beats$\cdot min^{-1} \cdot Hz^{-1}$ (means ± SD; $P <$ 0.01) without affecting the corner frequency or pure delay. In the sympathetic stimulation group (n = 7), we stimulated the right postganglionic cardiac sympathetic nerve for 20 min using binary white noise (0–5 Hz). The transfer function from sympathetic stimulation to HR approximated a second-order low-pass filter with pure delay. ANG II slightly attenuated the dynamic gain from 10.8 ± 2.6 to 10.2 ± 3.1 beats$\cdot min^{-1} \cdot Hz^{-1}$ (P = 0.049) without affecting the natural frequency, damping ratio, or pure delay. The disproportional suppression of the dynamic vagal and sympathetic regulation of HR would result in a relative sympathetic predominance in the presence of ANG II. The reduced high-frequency component of HR variability in patients with cardiovascular diseases, such as myocardial infarction and heart failure, may be explained in part by the peripheral effects of ANG II on the dynamic autonomic regulation of HR.

systems analysis; transfer function; heart rate variability; cardiac sympathetic nerve activity; rabbit

AUTONOMIC NERVOUS ACTIVITY changes dynamically during daily activity, and thus the dynamic heart rate (HR) regulation by the autonomic nervous system is physiologically important. The high-frequency (HF) component of HR variability (HRV) is thought to reflect primarily vagal nerve activity, because the vagal nerve can change the HR more quickly than the sympathetic nerve (1, 3, 14, 34). This does not mean, however, that the sympathetic system cannot affect the HF component. For example, an increase in background sympathetic tone augments the HR response to vagal stimulation, an effect that has been referred to as accentuated antagonism (20). In accordance with accentuated antagonism, selective cardiac sympathetic nerve stimulation augments the dynamic HR response to vagal stimulation (14). On the other hand, high plasma concentration of norepinephrine (NE) with no direct activation of the cardiac sympathetic nerve attenuates the dynamic HR response to vagal stimulation via an α-adrenergic mechanism (24). These results suggest that the sympathetic system can influence the HF component via complex interactions with the vagal system.

During systemic sympathetic activation, the renin-angiotensin system is activated through stimulation of β_1-adrenergic receptors on juxtaglomerular granular cells (8, 12). In such conditions as hypertension, myocardial ischemia, and heart failure, the renin-angiotensin system and the sympathetic nervous system are both activated (9, 35). Previous studies demonstrated that acute intravenous or intracerebroventricular administration (32) or chronic intravenous administration of angiotensin II (ANG II) modified the baroreflex control of HR in rabbits (5), possibly via a decrease in vagal tone and an increase in sympathetic tone to the heart. In the present study, we focused on the peripheral effects of ANG II and examined the effects of intravenous ANG II on the dynamic HR response to vagal or postganglionic cardiac sympathetic nerve stimulation. In a previous study from our laboratory where anesthetized cats were used, intravenous ANG II (10 $\mu g \cdot kg^{-1} \cdot h^{-1}$) attenuated myocardial interstitial acetylcholine (ACh) release in response to vagal nerve stimulation (17); therefore, we hypothesized that intravenous ANG II at this dose would attenuate the dynamic HR response to vagal nerve stimulation. On the other hand, a previous study from our laboratory where anesthetized rabbits were used demonstrated that intravenous ANG II at a similar dose of 6 $\mu g \cdot kg^{-1} \cdot h^{-1}$ did not affect the peripheral arc transfer function estimated between renal sympathetic nerve activity and arterial pressure (AP) (13). Accordingly, we hypothesized that intravenous administration of ANG II would not modulate the dynamic sympathetic control of HR significantly. We focused on the relative effects of ANG II on the vagal and sympathetic HR regulations because the balance between vagal and sympathetic nerve activities would be a key to understanding the pathophysiology of several cardiovascular diseases.

MATERIALS AND METHODS

Surgical preparations. Animal care was performed in accordance with *Guideline Principles for the Care and Use of Animals in the Field of Physiological Sciences*, which has been approved by the Physiological Society of Japan. All experimental protocols were reviewed and approved by the Animal Subjects Committee at the National Cardiovascular Center. Twenty-one Japanese white rabbits weighing 2.4–3.4 kg were anesthetized with intravenous injections (2 ml/kg) of a mixture of urethane (250 mg/ml) and α-chloralose (40 mg/ml) and mechanically ventilated with oxygen-enriched room air. A double-lumen catheter was inserted into the right femoral vein, and a supplemental dose of the anesthetics was given continuously (0.5–1.0

Address for reprint requests and other correspondence: T. Kawada, Dept. of Cardiovascular Dynamics, Advanced Medical Engineering Center, National Cardiovascular Center Research Institute, 5-7-1 Fujishirodai, Suita, Osaka 565-8565, Japan (e-mail: torukawa@res.ncvc.go.jp).

$ml \cdot kg^{-1} \cdot h^{-1}$). AP was monitored using a micromanometer catheter (Millar Instruments, Houston, TX) inserted into the right femoral artery. HR was determined from the electrocardiogram using a cardiotachometer. Sinoaortic denervation and vagotomy were performed bilaterally to minimize reflex changes in efferent sympathetic nerve activity. The left and right cardiac sympathetic nerves were exposed using a midline thoracotomy and sectioned (16). In the vagal stimulation group, a pair of bipolar stainless steel wire electrodes was attached to the cardiac end of the sectioned right vagal nerve for stimulation. A pair of stainless steel wire electrodes was attached to the proximal end of the sectioned right cardiac sympathetic nerve for recording efferent cardiac sympathetic nerve activity (CSNA). In the sympathetic stimulation group, a pair of bipolar stainless steel wire electrodes was attached to the cardiac end of the sectioned right sympathetic nerve for stimulation. Efferent CSNA was recorded from the proximal end of the sectioned left cardiac sympathetic nerve. The preamplified nerve signal was band-pass filtered between 150 and 1,000 Hz. The signal was then full-wave rectified and low-pass filtered with a cut-off frequency of 30 Hz to quantify the nerve activity. Both the stimulation and recording electrodes were fixed to the nerve by addition-curing silicone glue (Kwik-Sil; World Precision Instruments, Sarasota, FL). We confirmed that the recorded CSNA was mainly postganglionic by observing the disappearance of CSNA following intravenous administration of hexamethonium bromide (50 mg/kg) at the end of each experiment. The body temperature of the animal was maintained at 38°C with a heating pad throughout the experiment.

Protocols. In the vagal stimulation group (n = 7), the stimulation amplitude was adjusted (3–6 V) in each animal to yield a HR decrease of ~50 beats/min at 5-Hz tonic stimulation with a pulse duration of 2 ms. To estimate the transfer function from vagal stimulation to HR, a random vagal stimulus was applied for 10 min by altering the stimulus command every 500 ms at either 0 or 10 Hz according to a binary white noise signal. The input power spectral density was relatively constant up to 1 Hz, which covered the upper frequency range of interest with respect to the vagal transfer function in rabbits (26).

In the sympathetic stimulation group (n = 7), the stimulation amplitude was adjusted (1–3 V) in each animal to yield a HR increase of ~50 beats/min at 5-Hz tonic stimulation with a pulse duration of 2 ms. To estimate the transfer function from sympathetic stimulation to HR, a random sympathetic stimulus was applied for 20 min by altering the stimulus command every 2 s at either 0 or 5 Hz according to a binary white noise signal. The input power spectral density was relatively constant up to 0.25 Hz, which covered the upper frequency range of interest with respect to the sympathetic transfer function in rabbits (15).

In both the vagal stimulation and sympathetic stimulation groups, the dynamic HR response to nerve stimulation was first recorded under conditions of continuous intravenous infusion of physiological saline solution ($1\ ml \cdot kg^{-1} \cdot h^{-1}$). After the control data were recorded, nerve stimulation was stopped and ANG II was intravenously administered at $10\ \mu g \cdot kg^{-1} \cdot h^{-1}$ ($1\ ml \cdot kg^{-1} \cdot h^{-1}$ of 10 μg/ml solution) instead of the physiological saline solution. After 15 min, we repeated the random stimulation of the vagal or sympathetic nerve while continuing the intravenous injection of ANG II. We used the same binary white noise sequence for the control and ANG II conditions in each animal and changed the sequence for different animals.

In a supplemental protocol (n = 7), we examined the time effect on the estimation of the sympathetic transfer function. The 20-min random sympathetic stimulation was repeated twice with an intervening interval of more than 20 min.

Data analysis. Data were digitized at 200 Hz using a 16-bit analog-to-digital converter and stored on the hard disk of a dedicated laboratory computer system. Prestimulation values of HR, AP, and CSNA were calculated by averaging data obtained during the 10 s immediately before nerve stimulation. The mean HR and AP values in response to nerve stimulation were calculated by averaging data obtained during the nerve stimulation period. The mean level of CSNA during the nerve stimulation period was not evaluated because contamination from stimulation artifacts could not be completely eliminated.

The transfer function from nerve stimulation to the HR response was estimated as follows. The input-output data pairs of nerve stimulation and HR were resampled at 10 Hz. To avoid the initial transition from no stimulation to random stimulation biased the transfer function estimation, data were processed only from 2 min after the initiation of random stimulation. In the vagal stimulation group, the data were divided into eight segments of 1,024 data points that half-overlapped with neighboring segments. In the sympathetic stimulation group, the data were divided into eight segments of 2,048 data points that half-overlapped with neighboring segments. For each segment, a linear trend was subtracted and a Hanning window was applied. We then performed a fast Fourier transformation to obtain the frequency spectra of the stimulation command [$X(f)$] and HR [$HR(f)$] (4). We calculated ensemble averages of the power spectral densities of the stimulation command [$S_{X \cdot X}(f)$] and HR [$S_{HR \cdot HR}(f)$] and the cross spectral density between the two signals [$S_{HR \cdot X}(f)$]. Finally, we obtained the transfer function [$H(f)$] from the nerve stimulation to HR response using the following equation (23):

$$H(f) = \frac{S_{HR \cdot X}(f)}{S_{X \cdot X}(f)}$$

To quantify the linear dependence of the HR response to vagal or sympathetic nerve stimulation, we estimated the magnitude-squared coherence function [$Coh(f)$] using the following equation (23):

$$Coh(f) = \frac{|S_{HR \cdot X}(f)|^2}{S_{X \cdot X}(f) \cdot S_{HR \cdot HR}(f)}$$

The coherence function ranges zero and unity and indicates a frequency-domain measure of linear dependence between input and output variables.

Because previous studies found that the transfer function from vagal stimulation to HR approximated a first-order low-pass filter with pure delay (14, 24), we determined the parameters of the vagal transfer function using the following model:

$$H_{vagus}(f) = -\frac{K}{1 + \frac{f}{f_C} j} e^{-2\pi f j L}$$

where K is dynamic gain (in $beats \cdot min^{-1} \cdot Hz^{-1}$), f_C is the corner frequency (in Hz), and L is pure delay (in s). Variables f and j represent frequency and an imaginary unit, respectively. The minus sign in the right side of the equation corresponds to the negative HR response to vagal stimulation.

Because previous studies suggested that the transfer function from sympathetic stimulation to HR approximated a second-order low-pass filter with pure delay (14, 28), we determined the parameters of the sympathetic transfer function using the following model:

$$H_{symp}(f) = \frac{K}{1 + 2\zeta \frac{f}{f_N} j + \left(\frac{f}{f_N} j\right)^2} e^{-2\pi f j L}$$

where K is dynamic gain (in $beats \cdot min^{-1} \cdot Hz^{-1}$), f_N is the natural frequency (in Hz), ζ is the damping ratio, and L is pure delay (in s).

Because deviation of the model transfer function [$H_{model}(f)$] from the estimated transfer function [$H_{est}(f)$] would affect the transfer function parameters, we assessed the goodness of fit using the following equation:

$$\text{Goodness of Fit (\%)} = 100 \times \left[1 - \left(\sum_{m=1}^{N} \frac{|H_{model}(f) - H_{est}(f)|^2}{m}\right) \Big/ \left(\sum_{m=1}^{N} \frac{|H_{est}(f)|^2}{m}\right)\right]$$

$$f = f_0 \times m$$

where f_0, m, and N represent the fundamental frequency of the Fourier transformation, a frequency index, and the number of data points used for the fitting, respectively. When $H_{model}(f)$ is zero for all of the frequencies, the goodness of fit is zero. When $H_{model}(f)$ equals $H_{est}(f)$ for all of the frequencies, the goodness of fit is 100%.

To facilitate intuitive understanding of the dynamic characteristics described by the transfer function (see Appendix A for details), we calculated the step response from the corresponding transfer function as follows. An impulse response of the system was calculated using the inverse Fourier transformation of the estimated transfer function. The step response was then obtained from the time integral of the impulse response. The steady-state response was calculated by averaging the last 10 s of data from the step response. The 80% rise time for the sympathetic step response or the 80% fall time for the vagal step response was estimated as the time at which the step response reached 80% of the steady-state response.

Statistics. All data are presented as means and SD values. Mean values of HR, AP, and CSNA as well as parameters of the transfer functions and step responses were compared between the control and ANG II conditions using paired *t*-tests. Differences were considered significant when $P < 0.05$ (11).

RESULTS

Typical recordings of the vagal stimulation command, HR, and AP obtained under control and ANG II conditions are shown in Fig. 1*A*. The random vagal stimulation began at 60 s. The HR decreased in response to the random vagal stimulation. ANG II, which did not affect the prestimulation baseline HR, attenuated the magnitude of the vagal stimulation-induced variations in HR. ANG II increased the AP both before and during the vagal stimulation. ANG II did not change the prestimulation or poststimulation CSNA (Fig. 1*B*).

As shown in Table 1, ANG II did not affect the mean HR before stimulation of the vagal nerve, whereas it significantly increased the mean HR during the vagal stimulation period. ANG II attenuated the reduction in HR, which was calculated as the difference between the prestimulation HR and the mean HR observed during the vagal stimulation period. ANG II significantly increased the mean AP both before and during the vagal stimulation period. ANG II did not affect the mean level of pre- or poststimulation CSNA significantly.

Figure 2*A* illustrates the averaged transfer functions from vagal stimulation to HR obtained under the control and ANG II conditions. In the gain plots, the transfer gain was relatively constant for frequencies below 0.1 Hz and decreased as the frequency increased above 0.1 Hz. ANG II decreased the transfer gain for all of the investigated frequencies, resulting in

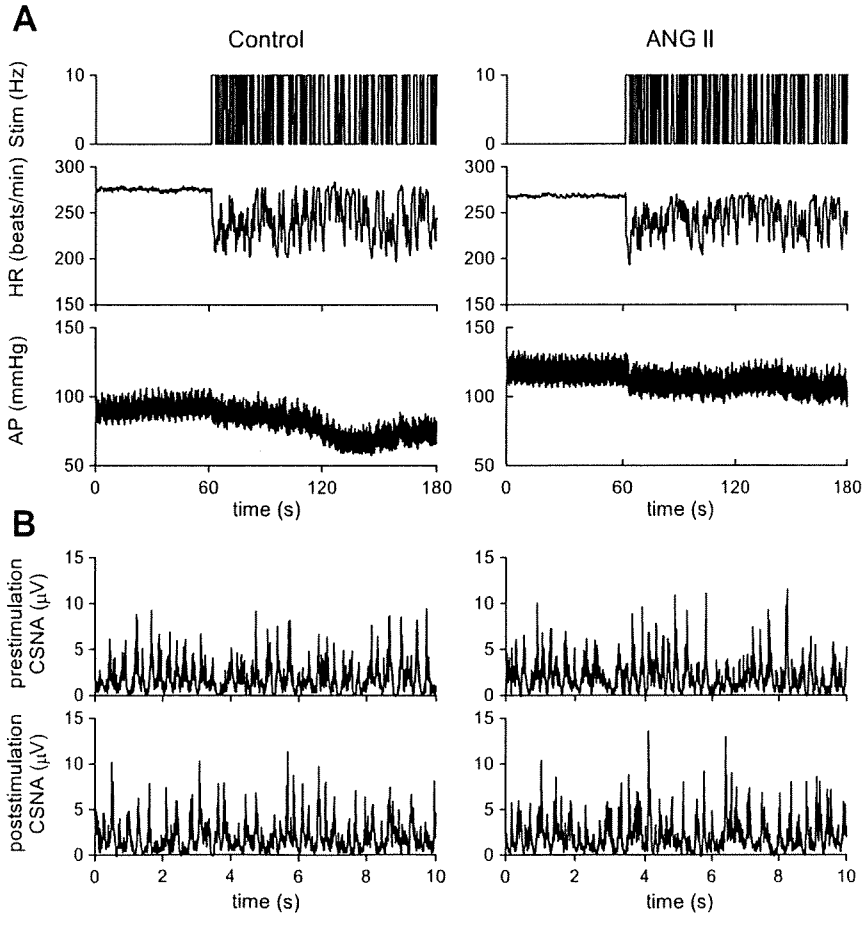

Fig. 1. *A*: representative recordings of vagal nerve stimulation (Stim), the heart rate (HR), and arterial pressure (AP). The *left* and *right* panels show recordings obtained before and during intravenous administration of angiotensin II (ANG II; 10 $\mu g \cdot kg^{-1} \cdot h^{-1}$), respectively. The amplitude of the HR variation in response to vagal stimulation was smaller in the presence of ANG II compared with results obtained without ANG II. *B*: representative recordings of cardiac sympathetic nerve activity (CSNA) under prestimulation baseline and poststimulation conditions. ANG II did not affect the CSNA significantly.

Table 1. *Mean values for HR, AP, and CSNA obtained using the vagal stimulation protocol*

	Control	ANG II	*P* Value
HR, beats/min			
Prestimulation	278±21	281±31	0.60
During stimulation	232±19	245±26*	0.046
Difference‡	−46±6	−37±10†	0.0017
AP, mmHg			
Prestimulation	91±23	127±17†	0.0057
During stimulation	85±24	118±19†	0.0055
Difference‡	−6.3±9.2	−9.2±8.6	0.34
CSNA, μV			
Prestimulation	1.21±0.38 (100%)	1.19±0.46 (98±15%)	0.82
Poststimulation	1.27±0.42 (105±8%)	1.20±0.55 (98±27%)	0.59

Data are means ± SD values; $n = 7$. HR, heart rate; AP, arterial pressure; CSNA, cardiac sympathetic nerve activity. ‡The difference was calculated by subtracting the prestimulation value from the value obtained during the vagal stimulation period in each animal. *$P < 0.05$ and †$P < 0.01$ based on a paired *t*-test. Exact *P* values are also shown.

a parallel downward shift in the gain plot. In the phase plots, the phase approached $-\pi$ radians at 0.01 Hz and the lag became larger as the frequency increased. ANG II did not alter the phase characteristics significantly. In the coherence plots, the coherence value was close to unity in the frequency range from 0.01 to 0.8 Hz. The sharp variation around 0.6 Hz corresponds to the frequency of the artificial ventilation. Figure 2*B* depicts the HR step responses calculated from the corresponding transfer functions. ANG II significantly attenuated the steady-state response without affecting the response speed.

As shown in Table 2, ANG II significantly attenuated the dynamic gain of the vagal transfer function to 76.1 ± 8.5% of the control value without affecting the corner frequency or pure delay. The goodness of fit to the first-order low-pass filter did not differ between the control and ANG II conditions. In the HR step response, ANG II significantly attenuated the steady-state response without affecting the 80% fall time.

Typical recordings of the sympathetic stimulation command, HR, and AP obtained under control and ANG II conditions are shown in Fig. 3*A*. The random sympathetic stimulation began at 60 s. HR increased in response to random sympathetic stimulation. ANG II did not affect the prestimulation baseline HR. The magnitude of the HR variation in response to sympathetic stimulation did not change significantly. ANG II increased the AP both before and during the sympathetic stimulation. ANG II did not change the pre- or poststimulation CSNA significantly (Fig. 3*B*).

As shown in Table 3, ANG II did not affect the mean HR before or during the period of sympathetic stimulation. ANG II did not affect the increase in HR, calculated as the difference between the prestimulation HR and the mean HR in response to sympathetic stimulation. ANG II significantly increased the mean AP both before and during the sympathetic stimulation period. ANG II did not affect the mean level of pre- or poststimulation CSNA significantly.

Figure 4*A* illustrates the averaged transfer functions from sympathetic stimulation to HR obtained under control and ANG II conditions. In the gain plots, the transfer gain decreased as the frequency increased. ANG II did not change the transfer gain markedly. In the phase plots, the phase approached zero radians at 0.01 Hz and increasingly lagged as the frequency increased. ANG II did not affect the phase characteristics significantly. The coherence value was above 0.9 for the frequency range below 0.1 Hz and decreased in the frequency range above 0.1 Hz. Figure 4*B* depicts the HR step responses calculated from the corresponding transfer functions. ANG II did not affect the steady-state response or the response speed.

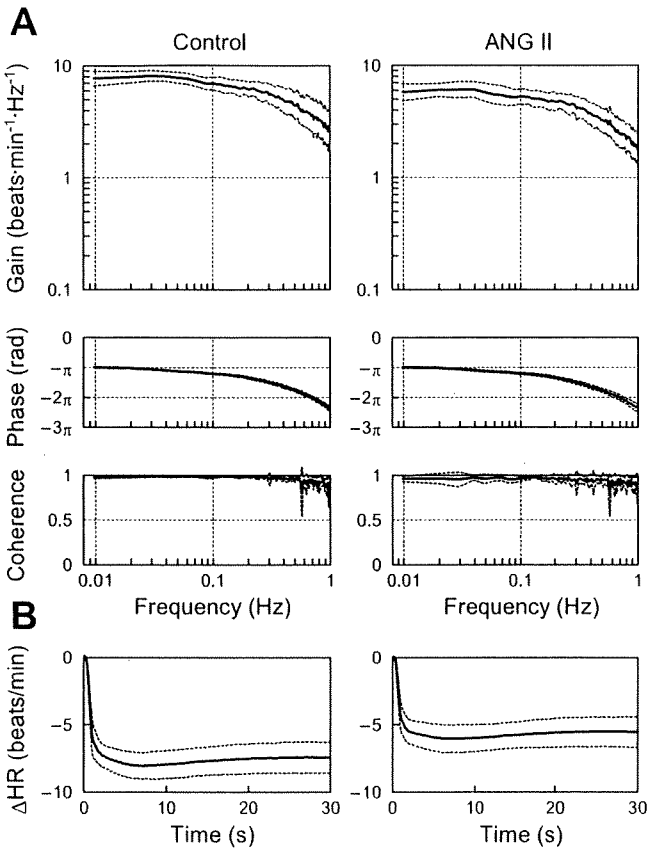

Fig. 2. *A*: averaged transfer functions from vagal nerve stimulation to the HR response obtained before and during intravenous administration of ANG II. Gain plots (*top*), phase plots (*middle*), and coherence plots (*bottom*) are shown. ANG II caused a parallel downward shift in the gain plot. ANG II did not affect the phase plot or coherence plot significantly. *B*: step responses of the HR to a unit change in the vagal stimulation calculated from the corresponding transfer functions. ANG II significantly attenuated the step response of the HR. ΔHR, changes in heart rate. Solid lines indicate mean, and dashed lines indicate mean ± SD.

Table 2. *Effects of ANG II on the parameters of the transfer function and the step response relating to the dynamic vagal control of HR*

	Control	ANG II	*P* Value
Dynamic gain, beats·min^{-1}·Hz^{-1}	7.6±0.9	5.8±0.9*	0.00042
Corner frequency, Hz	0.39±0.12	0.36±0.10	0.12
Pure delay, s	0.48±0.04	0.47±0.06	0.82
Goodness of fit, %	98.8±0.4	98.6±0.8	0.63
Steady-state response, beats/min	−7.4±1.1	−5.6±1.1*	0.0011
80% Fall time	1.31±0.31	1.33±0.37	0.60

Data are means ± SD values; $n = 7$. *$P < 0.01$ based on a paired *t*-test. Exact *P* values are also shown.

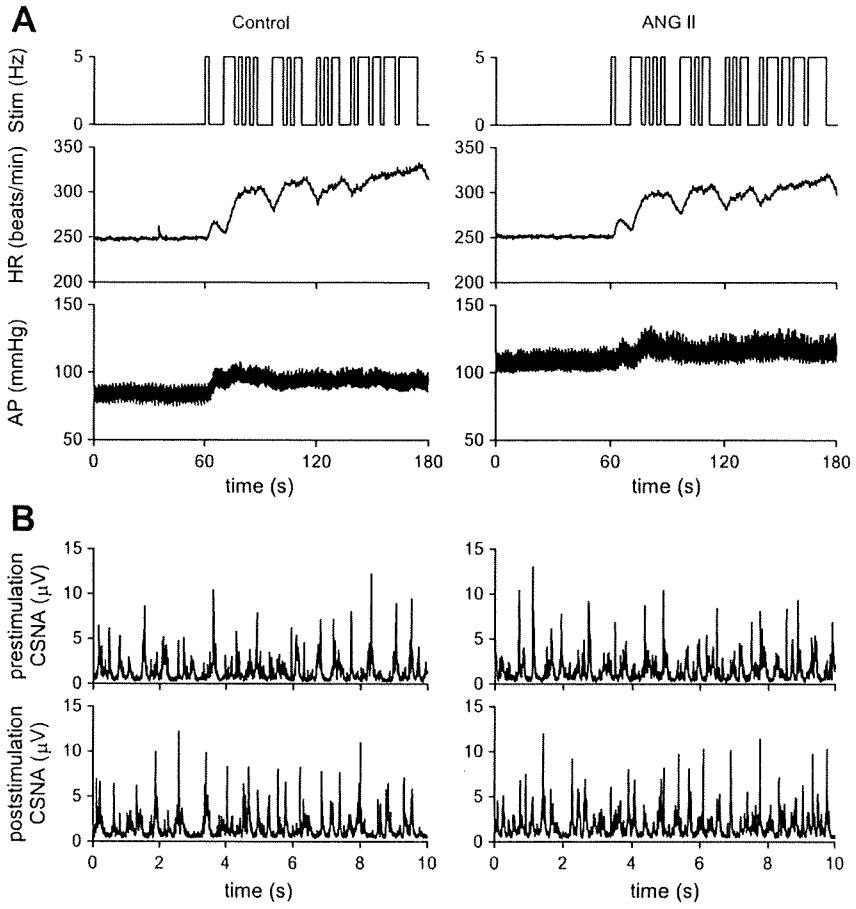

Fig. 3. *A*: representative recordings of cardiac sympathetic nerve stimulation (Stim), HR, and AP. The *left* and *right* panels show the recordings before and during intravenous administration of ANG II (10 $\mu g \cdot kg^{-1} \cdot h^{-1}$), respectively. The amplitude of the HR variation during sympathetic stimulation was unchanged by the addition of ANG II. *B*: representative recordings of CSNA under prestimulation baseline and poststimulation conditions. ANG II did not affect the CSNA significantly.

As shown in Table 4, ANG II slightly attenuated the dynamic gain of the sympathetic transfer function to 92.5 ± 8.9% of the value observed under control conditions. ANG II did not affect the natural frequency, damping ratio, or pure delay. The goodness of fit to the second-order low-pass filter did not differ between the control and ANG II conditions. In the HR step response, ANG II did not affect the steady-state response or the 80% rise time. As shown in Table 5, there were no significant differences in the parameters of the sympathetic transfer function between repeated estimations with an intervening interval of more than 20 min.

Table 3. *Mean values for HR, AP, and CSNA obtained using the sympathetic stimulation protocol*

	Control	ANG II	*P* Value
HR, beats/min			
Prestimulation	267±16	261±19	0.21
During stimulation	317±26	311±23	0.063
Difference†	50±21	50±21	0.94
AP, mmHg			
Prestimulation	74±6	106±15*	0.0011
During stimulation	78±6	110±17*	0.0023
Difference†	4.7±3.6	4.1±5.4	0.71
CSNA, μV			
Prestimulation	0.91±0.71 (100%)	0.98±0.78 (99±19%)	0.22
Poststimulation	0.93±0.72 (101±4%)	1.02±0.81 (104±21%)	0.18

Data are means ± SD values; $n = 7$ except for CSNA data where $n = 5$. †The difference was calculated by subtracting the prestimulation value from the value obtained during the sympathetic stimulation period in each animal. *$P < 0.01$ based on a paired *t*-test. Exact *P* values are also shown.

DISCUSSION

Intravenous administration of ANG II at 10 $\mu g \cdot kg^{-1} \cdot h^{-1}$ increased AP but did not affect mean HR or mean CSNA during prestimulation baseline conditions (Tables 1 and 3), suggesting that ANG II at this dose did not affect the residual sympathetic tone to the heart significantly. ANG II significantly attenuated the dynamic gain of the transfer function from vagal stimulation to HR, whereas it only slightly attenuated that of the transfer function from sympathetic stimulation to HR (Tables 2 and 4).

Effects of ANG II on the transfer function from vagal stimulation to HR. ANG II attenuated the dynamic gain of the transfer function from vagal stimulation to HR without affecting the corner frequency or pure delay (Fig. 2 and Table 2). Several interventions can affect the dynamic gain of the vagal transfer function and significantly change the corner frequency. For example, inhibition of cholinesterase, which interferes with the rapid hydrolysis of ACh, augments the dynamic gain and decreases the corner frequency (29). Moreover, blockade of muscarinic K^+ channels, which interferes with fast, membrane-delimited signal transduction, has been shown to attenuate the dynamic gain and decrease the corner frequency (26).

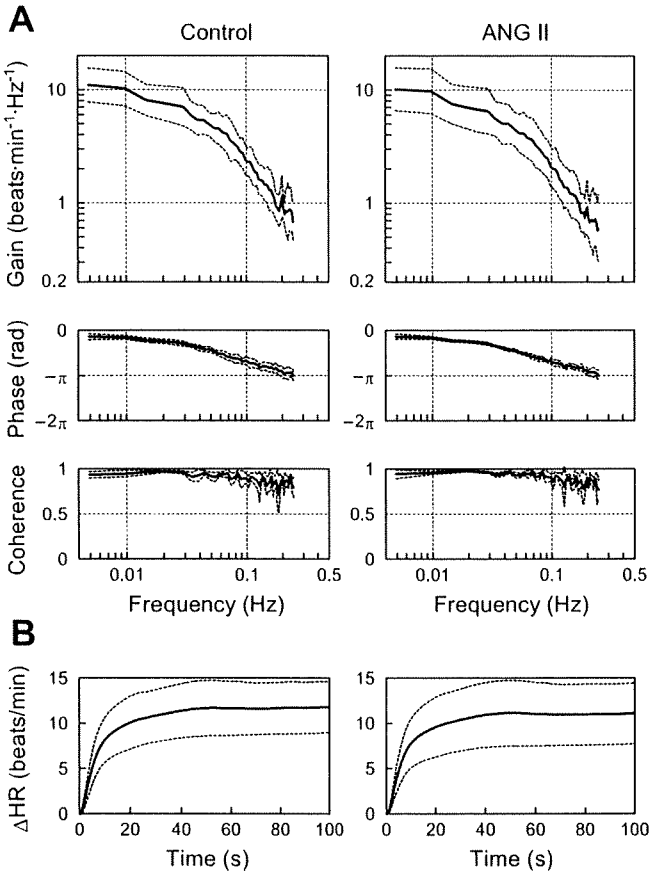

Fig. 4. *A*: averaged transfer functions from cardiac sympathetic nerve stimulation to the HR response obtained before and during intravenous administration of ANG II. Gain plots (*top*), phase plots (*middle*), and coherence plots (*bottom*) are shown. *B*: step responses of the HR to a unit change in the sympathetic stimulation calculated using the transfer functions. ΔHR, changes in heart rate. Solid lines indicate mean, and dashed lines indicate mean ± SD.

On the other hand, several other interventions have been shown to alter the dynamic gain of the vagal transfer function without changing the corner frequency. Concomitant cardiac sympathetic nerve stimulation or increased intracellular cyclic AMP levels augments the dynamic gain without affecting the corner frequency (14, 27), whereas β-adrenergic blockade or high plasma NE attenuates the dynamic gain without affecting the corner frequency (24, 25). Because α-adrenergic blockade nullifies its effects, high plasma NE probably functions via

Table 4. *Effects of intravenous ANG II administration on the parameters of the transfer function and the step response relating to the dynamic sympathetic control of HR*

	Control	ANG II	*P* Value
Dynamic gain, beats·min^{-1}·Hz^{-1}	10.8±2.6	10.2±3.1*	0.049
Natural frequency, Hz	0.069±0.009	0.065±0.006	0.090
Damping ratio	1.53±0.25	1.48±0.21	0.26
Pure delay, s	0.51±0.31	0.42±0.18	0.20
Goodness of fit, %	97.0±1.6	96.9±1.7	0.67
Steady-state response, beats/min	11.8±2.8	11.1±3.4	0.052
80% Rise time, s	17.2±4.7	16.8±4.5	0.62

Data are means ± SD; $n = 7$. *$P < 0.05$ based on a paired *t*-test. Exact *P* values are also shown.

Table 5. *Time effects on the parameters of the transfer function and the step response relating to the dynamic sympathetic control of HR*

	Control 1	Control 2	*P* Value
Dynamic gain, beats·min^{-1}·Hz^{-1}	9.1±1.7	8.6±2.4	0.37
Natural frequency, Hz	0.062±0.014	0.065±0.017	0.10
Damping ratio	1.36±0.22	1.34±0.28	0.75
Pure delay, s	0.65±0.32	0.56±0.25	0.12
Goodness of fit, %	95.8±4.0	97.3±2.2	0.32
Steady-state response, beats/min	9.8±2.0	9.5±2.8	0.55
80% Rise time, s	15.7±3.4	14.4±3.8	0.37

Data are means ± SD; $n = 7$. Exact *P* values are shown.

α-adrenergic receptors on preganglionic and/or postganglionic vagal nerve terminals to limit ACh release during vagal stimulation (24). Our observation that ANG II attenuated the dynamic gain without affecting the corner frequency or pure delay is similar to the results observed with high plasma NE, suggesting that ANG II limits ACh release during vagal stimulation. Although estimated values of the corner frequency ranged from 0.1 to 0.4 among studies, the difference may be attributable to the difference in the input signal properties (see Appendix B for details).

Although Andrews et al. (2) reported that ANG II (500 ng/kg, iv bolus) did not inhibit vagally induced bradycardia in anesthetized ferrets, Potter (31) demonstrated that ANG II (5–10 μg, iv bolus; body weight not shown) attenuated vagally induced bradycardia in anesthetized dogs. The latter study also showed that the addition of ANG II (2–5 μg/25 ml) to an organ bath attenuated vagally induced bradycardia in isolated guinea-pig atria. In that study, ANG II did not attenuate ACh-induced bradycardia, suggesting that the inhibition of bradycardia by ANG II was due to an inhibition of ACh release from vagal nerve terminals (31). In a previous study, we confirmed that intravenous ANG II (10 μg·kg^{-1}·h^{-1}) attenuated myocardial interstitial ACh release in response to vagal nerve stimulation in anesthetized cats (17). The site of this inhibitory action was thought to be parasympathetic ganglia rather than postganglionic vagal nerve terminals, because losartan, an antagonist of the ANG II receptor subtype 1 (AT_1 receptor), abolished the inhibitory action of ANG II when it was administered intravenously but not when it was administered locally through a dialysis fiber. ANG II may also function at the coronary endothelium and produce a diverse range of paracrine effects (6). Although the exact mechanisms remain to be elucidated, intravenous ANG II inhibits ACh release and thereby attenuates the dynamic gain of the vagal transfer function without affecting the corner frequency or pure delay.

Although the observed attenuation of the dynamic HR response to vagal stimulation by ANG II is relatively small, it may have pathophysiological significance as follows. In a previous study, our laboratory has shown that chronic intermittent vagal stimulation significantly improved the survival of chronic heart failure rats after myocardial infarction (21). In that study, the vagal stimulation intensity was such that it reduced HR only by 20 to 30 beats/min (5–10%) in rats. Therefore, change in the vagal effects on the heart, even if relatively small, could affect the evolution of heart failure. Increased plasma or tissue levels of ANG II in heart failure

might attenuate vagal neurotransmission, contributing to the aggravation of disease states.

Effects of ANG II on the transfer function from sympathetic stimulation to HR. Although ANG II attenuated the dynamic gain of the transfer function from sympathetic stimulation to HR without affecting the natural frequency, damping ratio, or pure delay, the attenuating effect was not definitive because the effect was not significant on the steady-state response in the calculated step response (Fig. 4 and Table 4). There are conflicting reports about the effects of ANG II on sympathetic control of the heart. Starke (33) reported that ANG II (1 ng/ml) potentiated NE release in response to postganglionic sympathetic nerve stimulation in isolated rabbit hearts, whereas no effect on spontaneous or tyramine-induced NE output was observed. Farrell et al. (10) demonstrated that administration of ANG II (100 μM at 1 ml/min for 10 min; ~35–42 $\mu g \cdot kg^{-1}$) into right atrial ganglionated plexus neurons via a branch of the right coronary artery caused the release of catecholamine into the myocardial interstitial fluid of anesthetized dogs, suggesting that ANG II affects intrinsic cardiac neurons. In that study, the effect of ANG II on the catecholamine release induced by cardiac sympathetic nerve stimulation was not investigated. On the other hand, Lameris et al. (19) demonstrated that administration of ANG II (0.5 $ng \cdot kg^{-1} \cdot min^{-1}$ or 30 $ng \cdot kg^{-1} \cdot h^{-1}$) into the left anterior descending coronary artery of anesthetized pigs did not yield spontaneous NE release or enhance the NE release induced by cardiac sympathetic nerve stimulation. Cardiac ganglia derived from different species can demonstrate differences in phenotype for ANG II receptors, and this may impact on the resultant neurohumoral interactions. Dendorfer et al. (7) demonstrated that ANG II (0.3 to 1 μg/kg bolus) increased renal sympathetic nerve activity during ganglionic blockade in pithed rats, suggesting direct ganglionic excitation by ANG II. In the present study, because we stimulated the postganglionic cardiac sympathetic nerve, possible direct ganglionic excitation by ANG II might not have affected the dynamic sympathetic control of HR. In addition, postganglionic CSNA did not change significantly in our experimental conditions (Tables 1 and 3), indicating that the 10 $\mu g \cdot kg^{-1} \cdot h^{-1}$ dose of intravenous ANG II was not high enough to produce direct ganglionic excitation.

In isolated rabbit hearts, Peach et al. (30) demonstrated that ANG II (0.2 ng/ml) inhibited NE uptake. Starke (33) reported a higher dose of ANG II (10 μg/ml) to inhibit NE uptake. In a previous study from our laboratory, blockade of neuronal NE uptake using desipramine attenuated the dynamic gain, decreased the natural frequency, and increased the pure delay of the transfer function from sympathetic stimulation to HR (28). In the present study, however, neither the natural frequency nor the pure delay was changed by ANG II, suggesting that NE uptake was not inhibited. In an in vivo study using canine hearts, Lokhandwala et al. (22) demonstrated that ANG II (100 and 200 $ng \cdot kg^{-1} \cdot min^{-1}$ or 6 and 12 $\mu g \cdot kg^{-1} \cdot min^{-1}$ iv) did not affect the positive chronotropic effects of either postganglionic cardiac sympathetic nerve stimulation or intravenous NE infusion. In that study, ANG II enhanced the positive chronotropic effects of sympathetic nerve stimulation but not of intravenous NE infusion after blocking neuronal NE uptake with desipramine. The authors' interpretation of the results was that ANG II facilitated NE release in response to sympathetic nerve stimulation, whereas any effects of ANG II might be masked in animals with functioning neuronal NE uptake mechanisms (22). To make matters more complex, Lameris et al. (19) did not observe enhanced NE release during cardiac sympathetic stimulation in porcine hearts even after neuronal NE uptake was blocked with desipramine. Thus it appears that differences in species, ANG II doses, and experimental settings (in vivo vs. isolated hearts, intravenous vs. intracoronary administration, with or without the contribution of sympathetic ganglia) critically affected the experimental results. Therefore, we believe that assessing the relative effects of ANG II on the vagal and sympathetic systems is important to understand the pathophysiological roles of ANG II in the autonomic regulation of HR.

Limitations. Our results should be interpreted in the context of various experimental limitations. First, we obtained data from anesthetized animals. If the data had been obtained under conscious conditions, the results might have been different. Because we disabled the arterial baroreflexes and cut the autonomic efferent pathways, however, the anesthetics should not have markedly affected our results. Second, because we stimulated the postganglionic cardiac sympathetic nerve, the possible effects of ANG II on the sympathetic ganglia were not assessed. Further studies that stimulate the preganglionic cardiac sympathetic nerve with various doses of ANG II are required to determine the effects of ANG II on the cardiac sympathetic ganglionic transmission. Finally, ANG II may affect the autonomic regulation of HR chronically. Further studies focused on the effects of chronically elevated ANG II levels on the autonomic regulation of HR are required to elucidate the pathophysiological significance of elevated ANG II levels.

In conclusion, continuous intravenous administration of ANG II at a dose that did not induce direct cardiac sympathetic ganglionic excitation significantly attenuated the dynamic gain of the transfer function from vagal stimulation to HR. The attenuation of the transfer gain was observed uniformly in the frequency range under study, suggesting that ANG II can attenuate the HF component of HRV even when vagal outflow from the central nervous system remains unchanged. In addition, the same dose of ANG II did not markedly affect the dynamic gain of the transfer function from postganglionic sympathetic stimulation to HR. Although there remains a room for arguments relating to the different site of stimulation (preganglionic for vagal vs. postganglionic for sympathetic), possible disproportional suppression of the dynamic vagal and sympathetic regulation of HR likely results in a relative dominance of sympathetic control in the presence of ANG II. Because many neurohumoral elements remodel or adapt during the evolution of cardiac pathology (18), we cannot directly extrapolate the results of acute neurohumoral interactions observed in the present study to the chronic pathological situations. If we do so, however, the reduction of the HF component of HRV in patients with cardiovascular diseases, such as myocardial infarction and heart failure (34), may be partly explained by the peripheral effects of ANG II on the dynamic autonomic regulation of HR.

APPENDIX A

Meaning of a step response calculated from a transfer function. We calculated a step response from a transfer function relating to the vagal or sympathetic HR control. The calculated step response is useful for time-domain interpretation of the low-pass filter characteristics described by the frequency-domain transfer function but does not necessarily conform to an experimentally estimated step response because of the following reasons. The transfer function identifies the

linear input-output relationship of a given system around a mean input signal (5 Hz for vagal and 2.5 Hz for sympathetic stimulation in the present study). The step response is then calculated for a unit change in the input signal. If we perform a kind of experiment where we change the stimulation frequency from 4.5 to 5.5 Hz for the vagal system and from 2 to 3 Hz for the sympathetic system, the resultant step response is most likely close to the calculated step response. The ordinary experimental step response is, however, estimated by a step input in which the stimulation is completely turned off before the stimulation starts. The calculated step response and the ordinary experimental step response can conform only when the system is purely linear. Whenever nonlinearities exist such as threshold and saturation commonly observed in biological systems, the two step responses disagree. Conversely, information gained by the ordinary experimental step response has a limited ability to estimate the dynamic HR response unless the system is purely linear.

Once vagal or sympathetic transfer function is identified, an impulse response of the system is obtained by an inverse Fourier transform of the transfer function. We can estimate the dynamic HR response from a convolution of a input signal and the impulse response. Figure 5 represents typical data of measured HR and calculated HR based on the transfer function. Figure 5*A* is a continuation of the time series obtained under the control condition depicted in Fig. 1*A*. Figure 5*B* shows a scatter plot of measured HR versus calculated HR during dynamic vagal stimulation. The solid line indicates a linear regression line ($r^2 = 0.94$). Figure 5*C* is a continuation of the time series obtained under the control condition depicted in Fig. 3*A*. Figure 5*D* shows the scatter plot of measured HR versus calculated HR during dynamic sympathetic stimulation. The solid line indicates a linear regression line. Although a slight convex nonlinearity is noted between the measured HR and calculated HR, squared correlation coefficient is high ($r^2 = 0.89$). These results indicate that the transfer function can represent the dynamic HR response reasonably well.

APPENDIX B

Binary white noise versus Gaussian white noise. In a previous study from our laboratory (29), we reported a corner frequency of ~0.1 Hz for a transfer function from vagal stimulation to HR, which was distinctly different from the result of the present study. Possible explanation for the discrepancy is the difference in the input variance (or power) of vagal stimulation. In the previous study, we used a Gaussian white noise (GWN) with a mean stimulation frequency of 5 Hz and a SD of 2 Hz so that the input signal covered at most 98.8% (means ± 2.5 SD) of the Gaussian distribution when the actual stimulation frequency was limited between 0 and 10 Hz. The variance of the GWN signal is 4 Hz^2. In contrast, the 0–10 Hz binary white noise used in the present study has a variance of 25 Hz^2. Hence, the binary white noise has a merit of increasing the input variance over the GWN when the stimulation frequency is limited between 0 and 10 Hz. Increasing the

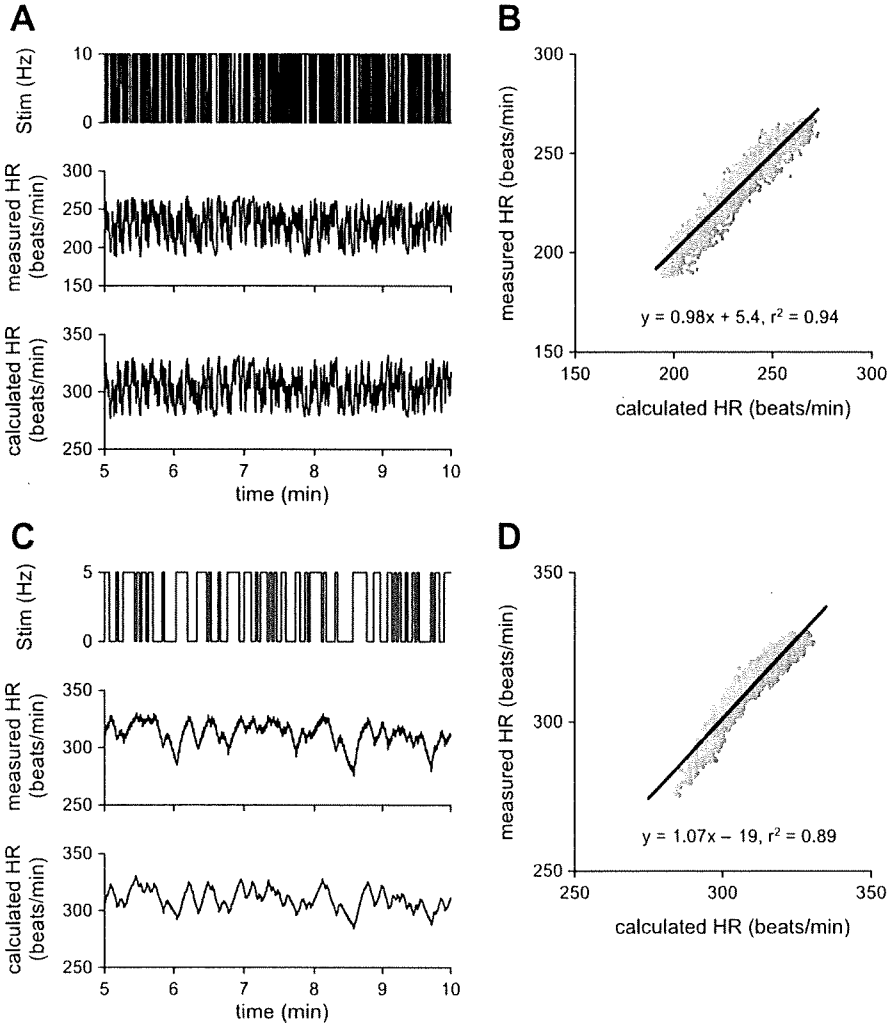

Fig. 5. *A*: data showing vagal stimulation (Stim), measured HR, and calculated HR based on the identified vagal transfer function of this animal. Time axis indicates the minutes after the initiation of random vagal stimulation (continuation of Fig. 1*A*). *B*: scatter plot between measured and calculated HR values. A solid line indicates a liner regression line. *C*: data showing sympathetic stimulation (Stim), measured HR, and calculated HR based on the identified sympathetic transfer function of this animal. Time axis indicates the minutes after the initiation of random sympathetic stimulation (continuation of Fig. 3*A*). *D*: scatter plot between measured and calculated HR values. A solid line indicates a linear regression line.

input variance is effective to increase the signal-to-noise ratio in the output signal and to improve the estimation of the transfer function.

In an earlier study on the transfer function analysis, Berger et al. (3) demonstrated that the roll-off of the vagal transfer function was gentle (i.e., the corner frequency was high) at high mean stimulatory rates and became more abrupt (i.e., the corner frequency was lower) with lower mean stimulatory rates. Although they attributed the difference in the roll-off characteristics to the difference in mean stimulatory rates, because they set the variance of input signal at ~1/4 of the mean stimulatory rates, which of the mean stimulatory rates or the input variance contributed to the determination of corner frequency seems inconclusive. Because there was no significant difference in the corner frequency between the vagal transfer functions estimated by GWNs of 5 ± 2 Hz and 10 ± 2 Hz (means ± SD) in a previous study from our laboratory (29), we speculate that the difference in the input variance rather than the mean stimulation frequency might have caused the different values of the corner frequency between the previous and the present results. This speculation requires further verification in future.

GRANTS

This study was supported by a Health and Labour Sciences Research Grant for Research on Advanced Medical Technology; a Health and Labour Sciences Research Grant for Research on Medical Devices for Analyzing, Supporting, and Substituting the Function of the Human Body; Health and Labour Sciences Research Grants H18-Iryo-Ippan-023, H18-Nano-Ippan-003, and H19-Nano-Ippan-009 from the Ministry of Health, Labour and Welfare of Japan; and the Industrial Technology Research Grant Program from the New Energy and Industrial Technology Development Organization of Japan.

REFERENCES

1. **Akselrod S, Gordon D, Ubel FA, Shannon DC, Berger AC, Cohen RJ.** Power spectrum analysis of heart rate fluctuation: a quantitative probe of beat-to-beat cardiovascular control. *Science* 213: 220–222, 1981.
2. **Andrews PL, Dutia MB, Harris PJ.** Angiotensin II does not inhibit vagally-induced bradycardia or gastric contractions in the anaesthetized ferret. *Br J Pharmacol* 82: 833–837, 1984.
3. **Berger RD, Saul JP, Cohen RJ.** Transfer function analysis of autonomic regulation. I. Canine atrial rate response. *Am J Physiol Heart Circ Physiol* 256: H142–H152, 1989.
4. **Brigham EO.** FFT transform applications. In: *The Fast Fourier Transform and Its Applications*. Englewood Cliffs, NJ: Prentice-Hall, 1988, p. 167–203.
5. **Brooks VL.** Chronic infusion of angiotensin II resets baroreflex control of heart rate by an arterial pressure-independent mechanism. *Hypertension* 26: 420–424, 1995.
6. **Castillo-Hernandez JR, Rubio-Gayosso I, Sada-Ovalle I, Garcia-Vazquez A, Ceballos G, Rubio R.** Intracoronary angiotensin II causes inotropic and vascular effects via different paracrine mechanisms. *Vascul Pharmacol* 41: 147–158, 2004.
7. **Dendorfer A, Thornagel A, Raasch W, Grisk O, Tempel K, Dominiak P.** Angiotensin II induces catecholamine release by direct ganglionic excitation. *Hypertension* 40: 348–354, 2002.
8. **DiBona GF.** Physiology in perspective: the wisdom of the body. Neural control of the kidney. *Am J Physiol Regul Integr Comp Physiol* 289: R633–R641, 2005.
9. **Diz DI, Averill DB.** Angiotensin II/autonomic interactions. In: *Primer on the Autonomic Nervous System*, edited by Robertson D, Biaggioni I, Burnstock G, and Low PA. San Diego: Elsevier Academic Press, 2004, p. 168–171.
10. **Farrell DM, Wei CC, Tallaj J, Ardell JL, Armour JA, Hageman GR, Bradley WE, Dell'Italia LJ.** Angiotensin II modulates catecholamine release into interstitial fluid of canine myocardium in vivo. *Am J Physiol Heart Circ Physiol* 281: H813–H822, 2001.
11. **Glantz SA.** *Primer of Biostatistics* (5th ed.). New York: McGraw-Hill, 2002.
12. **Jackson EK.** Autonomic control of the kidney. In: *Primer on the Autonomic Nervous System*, edited by Robertson D, Biaggioni I, Burnstock G, and Low PA. San Diego: Elsevier Academic Press, 2004, p. 157–161.
13. **Kashihara K, Takahashi Y, Chatani K, Kawada T, Zheng C, Li M, Sugimachi M, Sunagawa K.** Intravenous angiotensin II does not affect dynamic baroreflex characteristics of the neural or peripheral arc. *Jpn J Physiol* 53: 135–143, 2003.
14. **Kawada T, Ikeda Y, Sugimachi M, Shishido T, Kawaguchi O, Yamazaki T, Alexander J Jr, Sunagawa K.** Bidirectional augmentation of heart rate regulation by autonomic nervous system in rabbits. *Am J Physiol Heart Circ Physiol* 271: H288–H295, 1996.
15. **Kawada T, Miyamoto T, Miyoshi Y, Yamaguchi S, Tanabe Y, Kamiya A, Shishido T, Sugimachi M.** Sympathetic neural regulation of heart rate is robust against high plasma catecholamine. *J Physiol Sci* 56: 235–245, 2006.
16. **Kawada T, Uemura K, Kashihara K, Jin Y, Li M, Zheng C, Sugimachi M, Sunagawa K.** Uniformity in dynamic baroreflex regulation of left and right cardiac sympathetic nerve activities. *Am J Physiol Regul Integr Comp Physiol* 284: R1506–R1512, 2003.
17. **Kawada T, Yamazaki T, Akiyama T, Li M, Zheng C, Shishido T, Mori H, Sugimachi M.** Angiotensin II attenuates myocardial interstitial acetylcholine release in response to vagal stimulation. *Am J Physiol Heart Circ Physiol* 293: H2516–H2522, 2007.
18. **Khan MH, Sinoway LI.** Congestive heart failure. In: *Primer on the Autonomic Nervous System*, edited by Robertson D, Biaggioni I, Burnstock G, and Low PA. San Diego: Elsevier Academic Press, 2004, p. 247–248.
19. **Lameris TW, de Zeeuw S, Duncker DJ, Alberts G, Boomsma F, Verdouw PD, van den Meiracker AH.** Exogenous angiotensin II does not facilitate norepinephrine release in the heart. *Hypertension* 40: 491–497, 2002.
20. **Levy MN.** Sympathetic-parasympathetic interactions in the heart. *Circ Res* 29: 437–445, 1971.
21. **Li M, Zheng C, Sato T, Kawada T, Sugimachi M, Sunagawa K.** Vagal nerve stimulation markedly improves long-term survival after chronic heart failure in rats. *Circulation* 109: 120–124, 2004.
22. **Lokhandwala MF, Amelang E, Buckley JP.** Facilitation of cardiac sympathetic function by angiotensin II: role of presynaptic angiotensin receptors. *Eur J Pharmacol* 52: 405–409, 1978.
23. **Marmarelis PZ, Marmarelis VZ.** The white noise method in system identification. In: *Analysis of Physiological Systems*. New York: Plenum, 1978, p. 131–221.
24. **Miyamoto T, Kawada T, Takaki H, Inagaki M, Yanagiya Y, Jin Y, Sugimachi M, Sunagawa K.** High plasma norepinephrine attenuates the dynamic heart rate response to vagal stimulation. *Am J Physiol Heart Circ Physiol* 284: H2412–H2418, 2003.
25. **Miyamoto T, Kawada T, Yanagiya Y, Inagaki M, Takaki H, Sugimachi M, Sunagawa K.** Cardiac sympathetic nerve stimulation does not attenuate dynamic vagal control of heart rate via α-adrenergic mechanism. *Am J Physiol Heart Circ Physiol* 287: H860–H865, 2004.
26. **Mizuno M, Kamiya A, Kawada T, Miyamoto T, Shimizu S, Sugimachi M.** Muscarinic potassium channels augment dynamic and static heart rate responses to vagal stimulation. *Am J Physiol Heart Circ Physiol* 293: H1564–H1570, 2007.
27. **Nakahara T, Kawada T, Sugimachi M, Miyano H, Sato T, Shishido T, Yoshimura R, Miyashita H, Inagaki M, Alexander J Jr, Sunagawa K.** Accumulation of cAMP augments dynamic vagal control of heart rate. *Am J Physiol Heart Circ Physiol* 275: H562–H567, 1998.
28. **Nakahara T, Kawada T, Sugimachi M, Miyano H, Sato T, Shishido T, Yoshimura R, Miyashita H, Inagaki M, Alexander J Jr, Sunagawa K.** Neuronal uptake affects dynamic characteristics of heart rate response to sympathetic stimulation. *Am J Physiol Regul Integr Comp Physiol* 277: R140–R146, 1999.
29. **Nakahara T, Kawada T, Sugimachi M, Miyano H, Sato T, Shishido T, Yoshimura R, Miyashita H, Sunagawa K.** Cholinesterase affects dynamic transduction properties from vagal stimulation to heart rate. *Am J Physiol Regul Integr Comp Physiol* 275: R541–R547, 1998.
30. **Peach MJ, Bumpus FM, Khairallah PA.** Inhibition of norepinephrine uptake in hearts by angiotensin II and analogs. *J Pharmacol Exp Ther* 167: 291–299, 1969.
31. **Potter EK.** Angiotensin inhibits action of vagus nerve at the heart. *Br J Pharmacol* 75: 9–11, 1982.
32. **Reid IA, Chou L.** Analysis of the action of angiotensin II on the baroreflex control of heart rate in conscious rabbits. *Endocrinology* 126: 2749–2756, 1990.
33. **Starke K.** Action of angiotensin on uptake, release and metabolism of ^{14}C-noradrenaline by isolated rabbit hearts. *Eur J Pharmacol* 14: 112–123, 1971.
34. **Task Force of the European Society of Cardiology, the North American Society of Pacing and Electrophysiology.** Heart rate variability: standards of measurement, physiological interpretation and clinical use. *Circulation* 93: 1043–1065, 1996.
35. **Zimmerman BG, Sybertz EJ, Wong PC.** Interaction between sympathetic and renin-angiotensin system. *J Hypertens* 2: 581–587, 1984.

Circ J 2009; **73:** 851–859

Servo-Controlled Hind-Limb Electrical Stimulation for Short-Term Arterial Pressure Control

Toru Kawada, MD; Shuji Shimizu, MD; Hiromi Yamamoto, MD*;
Toshiaki Shishido, MD; Atsunori Kamiya, MD; Tadayoshi Miyamoto, PhD**;
Kenji Sunagawa, MD†; Masaru Sugimachi, MD

Background: Autonomic neural intervention is a promising tool for modulating the circulatory system thereby treating some cardiovascular diseases.

Methods and Results: In 8 pentobarbital-anesthetized cats, it was examined whether the arterial pressure (AP) could be controlled by acupuncture-like hind-limb electrical stimulation (HES). With a 0.5-ms pulse width, HES monotonically reduced AP as the stimulus current increased from 1 to 5 mA, suggesting that the stimulus current could be a primary control variable. In contrast, the depressor effect of HES showed a nadir approximately 10 Hz in the frequency range between 1 and 100 Hz. Dynamic characteristics of the AP response to HES approximated a second-order low-pass filter with dead time (gain: −10.2±1.6 mmHg/mA, natural frequency: 0.040±0.004 Hz, damping ratio 1.80±0.24, dead time: 1.38±0.13 s, mean±SE). Based on these dynamic characteristics, a servo-controlled HES system was developed. When a target AP value was set at 20 mmHg below the baseline AP, the time required for the AP response to reach 90% of the target level was 38±10 s. The steady-state error between the measured and target AP values was 1.3±0.1 mmHg.

Conclusions: Autonomic neural intervention by acupuncture-like HES might provide an additional modality to quantitatively control the circulatory system. (*Circ J* 2009; **73:** 851–859)

Key Words: Proportional-integral controller; Transfer function

Because abnormality in the autonomic nervous system is often associated with cardiovascular diseases, treating cardiovascular diseases by autonomic neural interventions have attracted many researchers![1–6] Recently, autonomic neural interventions using electronic devices have again gained the focus of attention as a potential modality for treating cardiovascular diseases resistant to conventional therapeutics. To name a few, chronic vagal nerve stimulation dramatically improves the survival of chronic heart failure after myocardial infarction in rats![7] Chronic baroreceptor activation enhances the survival of pacing-induced heart failure in dogs![8] A recent version of a device-based treatment of hypertension in human is reported![9] A framework of electrical neural intervention is also effective to elevate arterial pressure (AP) against hypotensive events![10–13]

Aside from direct neural stimulation, electroacupuncture can modify autonomic balance, thereby treating cardiovascular diseases![14–16] Although one feature of the electroacupuncture might be its long-lasting effects, immediate cardiovascular responses to acupuncture-like stimulation are also observed in several experimental settings. For example, a 60-s manual acupuncture-like stimulation of a hind limb reduces renal or cardiac sympathetic nerve activity, causing hypotension and bradycardia in anesthetized rats![17,18] We have shown that electrical stimulation of a hind limb using acupuncture needles immediately resets the arterial baroreflex and reduces sympathetic nerve activity in anesthetized rabbits![19] Acupuncture-like hind-limb electrical stimulation (HES) induces immediate hypotension with changes in the relationship between cardiac and renal sympathetic nerve activities in anesthetized cats![20]

In the present study, we hypothesized that AP could be controlled by HES. Quantification of the dynamic input–output relationship between a given stimulus and the AP response is essential for artificially controlling AP![10–12] Accordingly, the first aim was to identify the dynamic input–output relationship between HES and the AP response. The second aim was to develop a feedback controller system that could reduce AP at a prescribed target level using HES.

Methods

Surgical Preparation

Animal care was provided in strict accordance with the *Guiding Principles for the Care and Use of Animals in the Field of Physiological Sciences,* approved by the Physiological Society of Japan. All protocols were approved by the Animal Subject Committee of the National Cardiovascular Center. Eight adult cats weighing from 2.3 to 4.3 kg were

(Received November 17, 2008; revised manuscript received December 10, 2008; accepted December 21, 2008; released online March 18, 2009)

*Department of Cardiovascular Dynamics, Advanced Medical Engineering Center, National Cardiovascular Center Research Institute, Suita, †Division of Cardiology, Department of Internal Medicine, Kinki University School of Medicine, Osakasayama, **Department of Physical Therapy, Faculty of Health Sciences, Morinomiya University of Medical Sciences, Osaka and ‡Department of Cardiovascular Medicine, Graduate School of Medical Sciences, Kyushu University, Fukuoka, Japan*

Mailing address: Toru Kawada, MD, Department of Cardiovascular Dynamics, Advanced Medical Engineering Center, National Cardiovascular Center Research Institute, 5-7-1 Fujishirodai, Suita 565-8565, Japan. E-mail torukawa@res.ncvc.go.jp

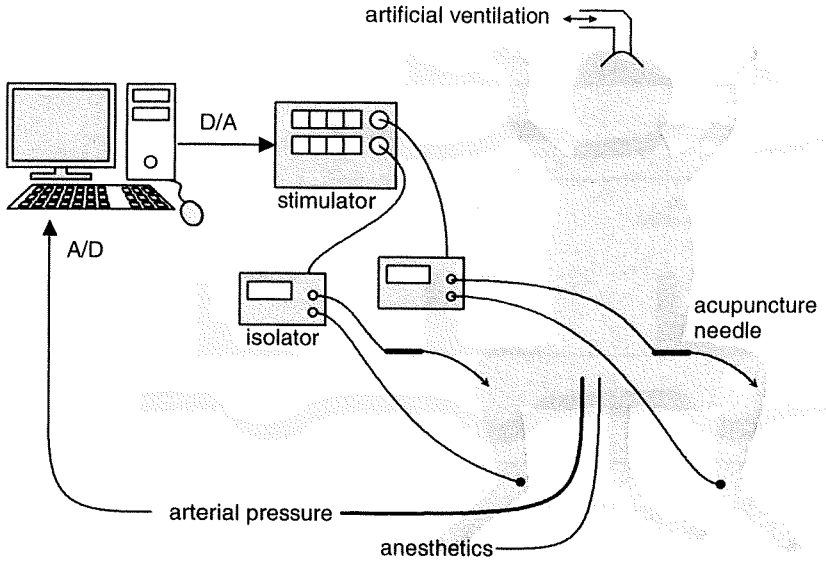

Figure 1. Experimental setup.

anesthetized by an intraperitoneal injection of pentobarbital sodium (30–35 mg/kg) and ventilated mechanically via a tracheal tube with oxygen-supplied room air. The depth of anesthesia was maintained with a continuous intravenous infusion of pentobarbital sodium (1–2 mg·kg^{-1}·h^{-1}) through a catheter inserted into the right femoral vein. Vecuronium bromide (0.5–1.0 mg·kg^{-1}·h^{-1}, iv) was given continuously to suppress muscular activity. AP was measured using a catheter-tip manometer inserted from the right femoral artery and advanced into the thoracic aorta.

HES

In the supine position, both hind limbs were lifted to obtain a better view of the lateral sides of the lower legs. An acupuncture needle with a diameter of 0.2 mm (CE0123, Seirin-Kasei, Shimizu, Japan) was inserted into a point below the knee joint just lateral to the tibia[20] A 23-gauge needle was inserted into the skin behind the ankle as the ground. HES was applied bilaterally via 2 independent isolators connected to an electrical stimulator (SEN 7203, Nihon Kohden, Tokyo, Japan) as shown in **Figure 1**. The pulse width was changed manually whereas the stimulus frequency and the stimulus current were controlled by a dedicated laboratory computer system. The electrical stimulation was started after the hemodynamic effects of needle insertion had disappeared, and the acupuncture needle remained inserted during each protocol.

Protocols

Protocol 1 (n=8) To quantify the AP response to HES as a function of stimulus current and pulse width, we fixed the stimulus frequency at 10 Hz and changed the stimulus current stepwise from 0 to 5 mA in 1-mA increments every minute. The 6-min current test was repeated with an intervening interval of 3–5 min using different pulse widths (0.1, 0.2, 0.5 and 1 ms). The order of the pulse-width settings was randomized across the animals.

Protocol 2 (n=8) To quantify the AP response to HES as a function of stimulus frequency and pulse width, we fixed the stimulus current at 3 mA and changed the stimulus frequency sequentially from 0 to 100 Hz (0, 1, 2, 5, 10, 15, 20, 50 and 100 Hz). Each stimulus frequency was maintained for 1 min. The 9-min frequency test was repeated with an intervening interval of 3–5 min using different pulse widths (0.1, 0.2, 0.5 and 1 ms). The order of the pulse-width settings was randomized across the animals.

Protocol 3 (n=8) To identify the dynamic input–output relationship between HES and the AP response, we randomly turned HES on and off every 2 s according to a binary white noise sequence for 30 min. The HES setting (0.5-ms pulse width, 10 Hz, 3 mA) was chosen to induce effective hypotension based on the preliminary results obtained from Protocols 1 and 2.

Protocol 4 (n=8) Based on the result of Protocol 3, we designed a feedback controller that could automatically adjust the stimulus frequency and the stimulus current for HES. The pulse width was fixed at 0.5 ms. To examine the performance of the feedback controller, we set a target AP value at 20 mmHg below the baseline AP and activated the feedback controller for 10 min.

The following 2 supplemental protocols were performed in 3 of the 8 cats: (1) we inserted 2 acupuncture needles into the triceps surae muscle with a distance of approximately 2.5 cm, and examined if changes in AP was associated with direct muscle stimulation (0.5-ms pulse width, 10 Hz, 3 mA). Both hind limbs were stimulated simultaneously using 2 independent isolators; and (2) we exposed the sciatic nerve after finishing Protocols 1 through 4, and examined if sectioning the sciatic nerve abolished the hemodynamic effects of HES. Unilateral HES was performed (0.5-ms pulse width, 10 Hz, 3 mA) before and after sectioning the ipsilateral sciatic nerve.

Data Analysis

In Protocols 1 and 2, the AP value was obtained by averaging the last 10-s data at each stimulus condition. In Protocol 1, the effect of stimulus current was assessed by changes in AP from the 0-mA stimulus condition for each pulse width. In Protocol 2, the effect of stimulus frequency was assessed by changes in AP from the 0-Hz stimulus condition for each pulse width.

In Protocol 3, the transfer function from HES to AP was estimated by means of an analysis for one-input, one-output systems. Data were first resampled at 10 Hz and segmented into 8 sets of 50%-overlapping bins of 4,096 points each. For each segment, a linear trend was subtracted and a

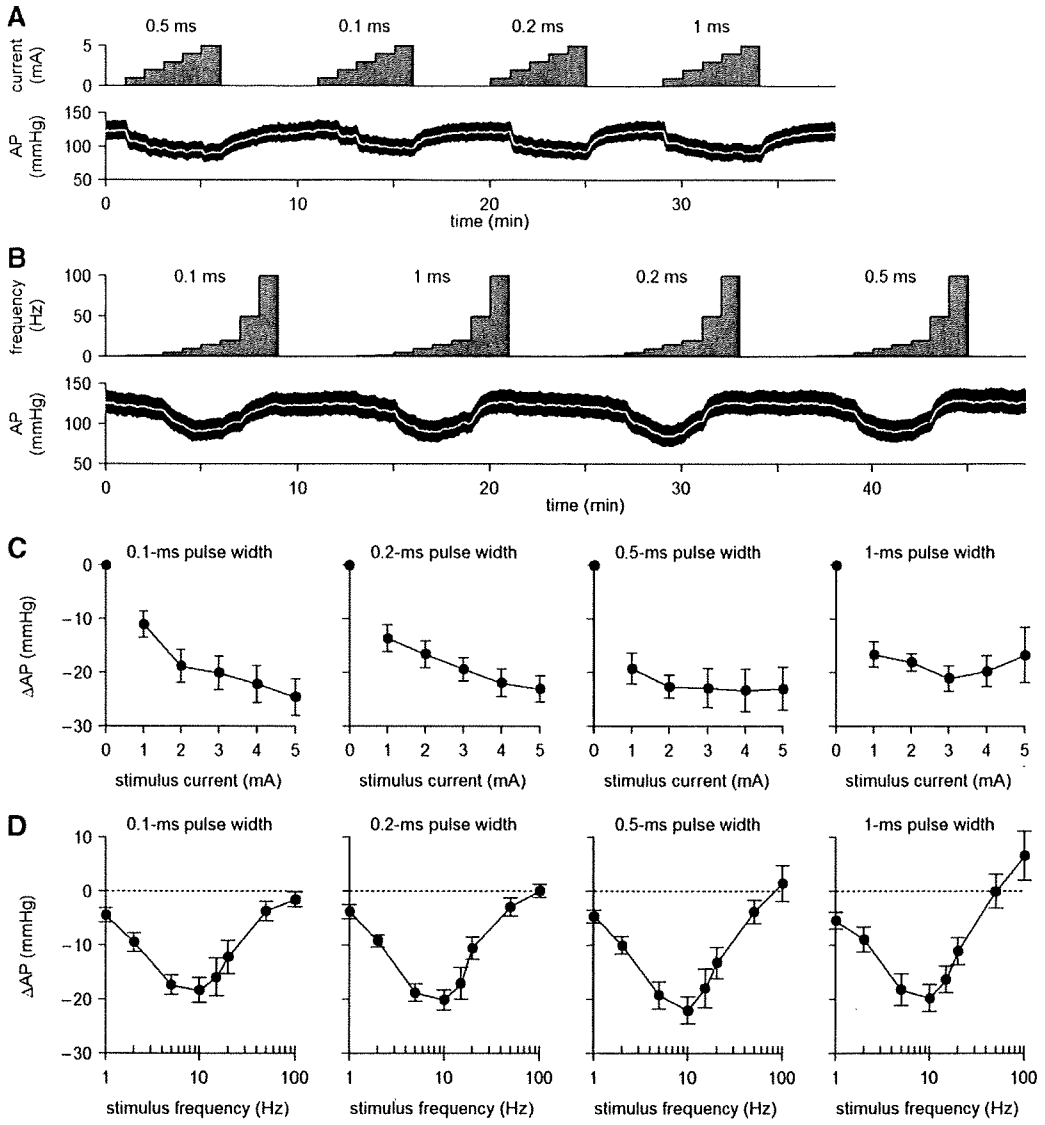

Figure 2. (**A**) Typical recordings of Protocol 1 showing the effects of stimulus current and pulse width on arterial pressure (AP). (**B**) Typical recordings of Protocol 2 showing the effects of stimulus frequency and pulse width on AP. The white lines in the AP traces indicate 2-s moving averaged data. (**C**) Changes in AP as a function of the stimulus current. AP decreased monotonously as the stimulus current increased ($P<0.05$). (**D**) Changes in AP as a function of the stimulus frequency. AP decreased more as the stimulus frequency increased from 1 to 10 Hz but the depressor effect became smaller when the stimulus frequency exceeded 10 Hz ($P<0.05$).

Hanning window was applied. Frequency spectra of the input and output were obtained via fast Fourier transformation. Next, the ensemble averages of input power spectral density [$Sxx(f)$], output power spectral density [$Syy(f)$], and cross spectral density between the input and output [$Syx(f)$] were calculated over the 8 segments. Finally, the transfer function from input to output [$H(f)$] was calculated as:[21]

$$H(f)=\frac{Syx(f)}{Sxx(f)} \quad (1)$$

To quantify the linear dependence between the input and output signals in the frequency domain, a magnitude-squared coherence function [$Coh(f)$] was also calculated as:[21]

$$Coh(f)=\frac{|Syx(f)|^2}{Sxx(f)Syy(f)} \quad (2)$$

In Protocol 4, the performance of the feedback controller was evaluated by the time required for the AP response to reach 90% of the target AP decrease and by the standard deviation of the steady-state error between the target and measured AP values during the last 5 min of the 10-min feedback control. These 2 values were calculated based on the 2-s moving averaged data of AP.

Statistical Analysis

All data are presented as mean and SE values. In Protocol 1, changes in AP were examined by 2-way repeated-measures analysis of variance (ANOVA) using the stimulus current as one factor and the pulse width as the other factor.[22] In Protocol 2, changes in AP were examined by 2-way repeated-measures ANOVA using the stimulus frequency as one factor and the pulse width as the other factor. Differences were considered significant when $P<0.05$.

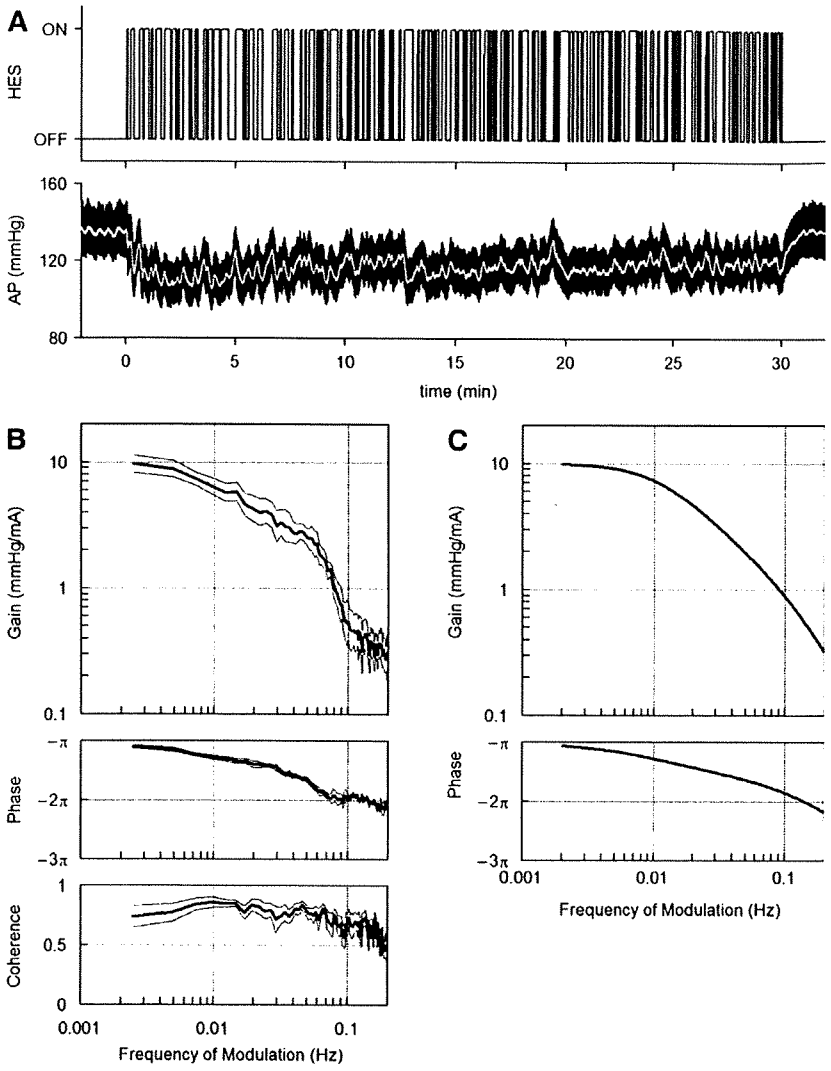

Figure 3. (**A**) Typical recordings of random hind-limb electrical stimulation (HES) and arterial pressure (AP) response. (**B**) Transfer function from HES to the AP response averaged from 8 cats. Thick and thin lines indicate mean and mean±SE values, respectively. (**C**) A model transfer function of the second-order low-pass filter with a lag time that mimics the transfer function from HES to AP.

Results

Relationship Between Stimulus Intensity and AP Response

Typical time series of Protocols 1 and 2 obtained from one animal are shown in **Figures 2A** and **B**, respectively. The pulse width was set in a random order. In Protocol 1, baseline AP obtained at the 0-mA stimulus condition was 118.4±5.4 mmHg across the animals. Changes in mean AP as a function of stimulus current are summarized in **Figure 2C**. The decrease in AP became greater as the stimulus current increased. The overall statistical analysis indicated that the effect of the stimulus current on the magnitude of AP decrease was significant whereas that of pulse width was not. There was no significant interaction effect between the stimulus current and the pulse width.

In Protocol 2, baseline AP at the 0-Hz stimulus condition was 117.6±5.9 mmHg across the animals. Changes in mean AP as a function of stimulus frequency are summarized in **Figure 2D**. The decrease in AP became greater as the stimulus frequency increased from 1 to 10 Hz but it became smaller when the stimulus frequency exceeded 10 Hz. At the pulse width of 1 ms, the stimulus frequency of 100 Hz even increased AP. The overall statistical analysis indicated that the effect of stimulus frequency on the magnitude of AP decrease was significant whereas that of pulse width was not. There was no significant interaction effect between the stimulus frequency and the pulse width.

Dynamic Characteristics of AP Response to HES

Figure 3A depicts a typical time series obtained from Protocol 3. HES was turned on and off randomly, which decreased the mean level of AP and also caused intermittent AP variations. When HES was finally turned off at 30 min, AP began to increase toward the prestimulation value. A long-lasting effect of HES was not observed in the present protocol. The white line in the AP trace represents the 2-s moving averaged data of AP.

The results of transfer function analysis are depicted in **Figure 3B**. In the gain plot, the magnitude of AP response relative to the HES input was plotted in the frequency domain. The gain value became smaller as the frequency increased, indicating the low-pass characteristics of the AP response to HES. In the phase plot, AP showed an out-of-phase relationship with HES at the lowest frequency (0.0024 Hz). The phase delayed more with increasing the frequency of modulation. The coherence value was approximately 0.7 in the frequency range below 0.06 Hz. The

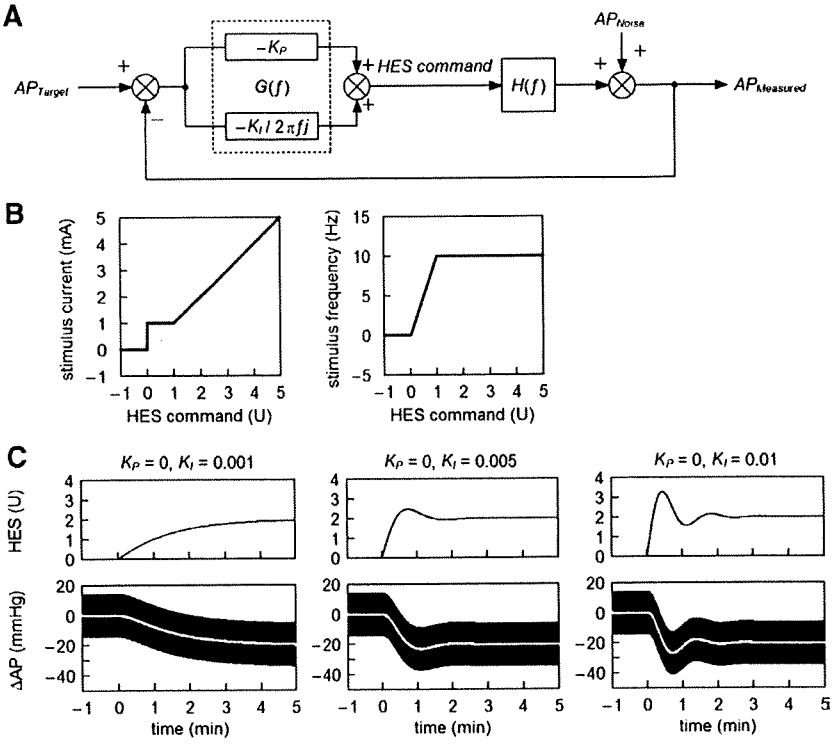

Figure 4. (A) A simplified diagram of the feedback controller utilized in the present study. AP_{Target}: target arterial pressure (AP); AP_{Noise}: noise in AP in terms of the control theory; $AP_{Measured}$: measured AP; $G(f)$: transfer function of the controller; $H(f)$: transfer function from hind-limb electrical stimulation (HES) to the AP response; K_P: proportional gain; K_I: integral gain; f and j denote the frequency and imaginary unit, respectively (see Appendix A for details). (B) Functions that convert the HES command into the stimulus current and the stimulus frequency. (C) Simulation results showing the feedback control of AP by HES. At time zero, the target AP was set at −20 mmHg. In the simulation, a sinusoidal wave (3 Hz, 15 mmHg in amplitude) was added to mimic the pulse pressure in AP. White lines indicate the 2-s moving averaged data of the simulated AP response.

coherence value became smaller in the frequency range above 0.1 Hz but still retained a value of 0.5, indicating that approximately half of the AP variation was explained by the HES input.

The general feature of the dynamic characteristics of the AP response to HES approximated what is known as a second order low-pass filter with a pure dead time, which is mathematically described as:

$$H(f)=\frac{-K}{1+2\zeta\frac{f}{f_N}j+\left(\frac{f}{f_N}j\right)^2}\exp(-2\pi fjL) \quad (3)$$

where K is the steady-state gain, f_N is the natural frequency, ζ is the damping ratio, and L is the pure dead time. When we performed an iterative non-linear least square fitting using a downhill Simplex method, K, f_N, ζ and L were estimated as 10.2±1.6 mmHg/mA, 0.040±0.004 Hz, 1.80±0.24 and 1.38± 0.13 s, respectively. A model transfer function shown in **Figure 3C** was drawn using K, f_N, ζ and L of 10 mmHg/mA, 0.04 Hz, 2 and 1 s, respectively.

Development of a Feedback Controller

We used a classical feedback controller to adjust the stimulus intensity of HES[23–25] In reference to **Figure 4A**, a HES command is determined based on a difference between measured and target AP values. $G(f)$ represents the transfer function of the controller with a proportional gain (K_P) and an integral gain (K_I). $H(f)$ indicates the model transfer function shown in **Figure 3C**. A detailed mathematical description of the controller is supplied in Appendix A.

To circumvent a threshold phenomenon in the stimulus current-AP response relationship (see Appendix B for details), the HES command (in an arbitrary unit) was transformed into the stimulus current (in mA) by a factor of 1 (**Figure 4B, Left**) only when the HES command exceeded unity. When the HES command was less than unity, the stimulus current was held at 1 mA and the HES command was transformed into the stimulus frequency (in Hz) by a factor of 10 (**Figure 4B, Right**). The stimulation was turned off when the HES command became negative.

Several sets of simulations were conducted using the model transfer function. The target AP was set at 20 mmHg below the baseline AP. To mimic the pulse pressure in AP, a 3-Hz sinusoidal wave (corresponding to the HR of 180 beats/min) with an amplitude of 15 mmHg (corresponding to the pulse pressure of 30 mmHg) was added to the AP signal. To avoid pulsatile variation in the HES command, we set the proportional gain at zero. Under this condition, when the integral gain was set at 0.001, AP decreased gradually and it took more than 3 min to reach the target AP (**Figure 4C, Left**). When the integral gain was set at 0.005, AP decreased more promptly and reached the target AP in less than 1 min (**Figure 4C, Center**). When the integral gain was set at 0.01, the AP response occurred more rapidly but showed significant oscillations before settling (**Figure 4C, Right**). Based on these simulation results, we set the proportional gain at zero and the integral gain at 0.005 for the actual feedback-control experiment in Protocol 4.

Performance of the Feedback Controller

Figure 5A demonstrates the AP regulation by HES obtained from 2 typical animals. The proportional and integral gains of the controller were not altered among the animals (ie, K_P=0, K_I=0.005). The white line in the AP trace indicates 2-s moving averaged data. The target AP was set at 20 mmHg below the AP value just before the application of HES. The feedback controller was activated for 10 min, which decreased AP at the target level. The HES command was individualized via the feedback mechanism. In the left panel of **Figure 5A**, the HES command gradually increased throughout the 10-min regulation. In the right panel of **Figure 5A**, the HES command was less than unity

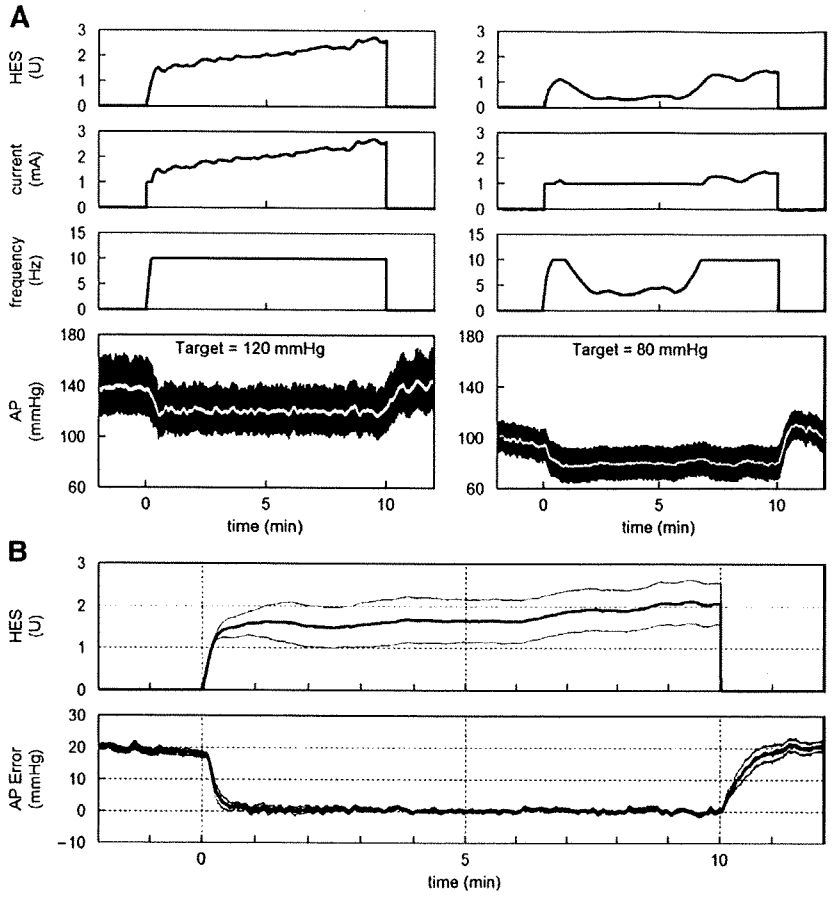

Figure 5. (**A**) Results of 10-min feedback control of arterial pressure (AP) by hind-limb electrical stimulation (HES) obtained from 2 cats. In each cat, the target AP was set at 20 mmHg below the baseline AP value. The current and frequency of HES were automatically adjusted to keep the AP at the target level. (**B**) HES command and the error signal between the target AP and measured AP averaged from 8 cats. The thick and thin lines indicate mean ± SE values, respectively.

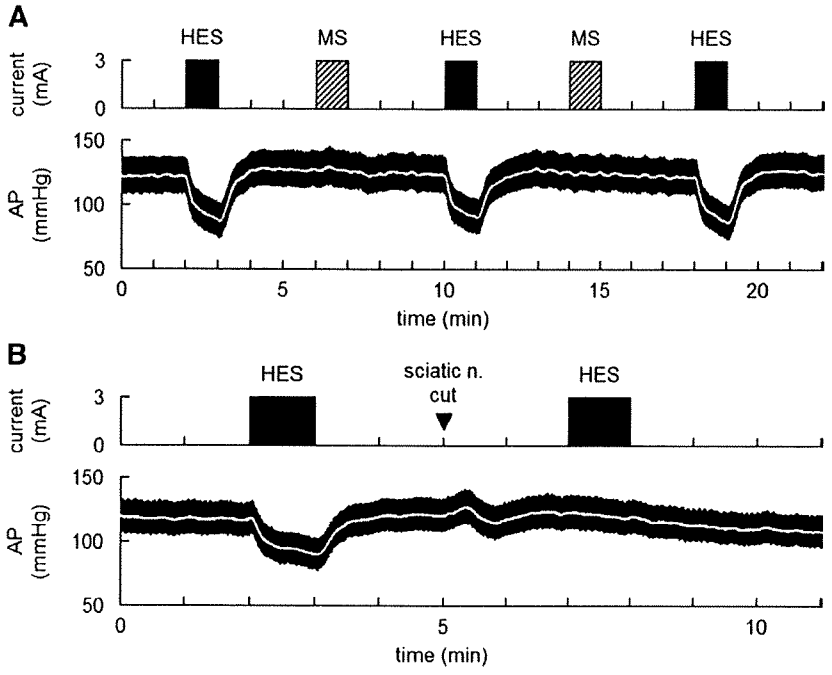

Figure 6. (**A**) Effects of electrical stimulation of the triceps surae muscle (MS) in comparison to hind-limb electrical stimulation (HES). Although muscle twitching was observed, there was no change in arterial pressure (AP) during MS. (**B**) Effects of sectioning the ipsilateral sciatic nerve on the HES-induced changes in AP. After the severance of the ipsilateral sciatic nerve, HES no longer produced significant hypotension.

from 1 to 7 min of the 10-min regulation. In this time period, the HES command altered the stimulus frequency rather than the stimulus current.

Mean and mean ± SE values of the HES command averaged from 8 animals are shown in the top panel of **Figure 5B**. There was a large variance in the HES command among the animals, suggesting inter-individual differences in the responsiveness to HES. The target AP was 102.5±5.6 mmHg across the animals. The error signal between the target AP and measured AP disappeared in less than 1 min (**Figure 5B**,

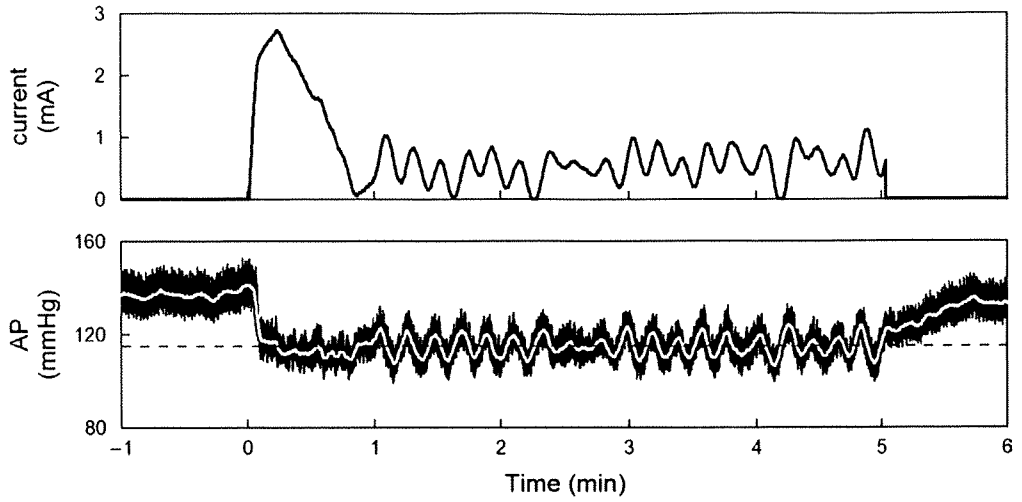

Figure 7. Typical recordings showing failure of controlling the intensity of the hind-limb electrical stimulation during the course of controller development. In this experimental run, only the stimulus current was controlled with a fixed stimulus frequency at 10 Hz. The controller showed on–off type controller behavior once the arterial pressure (AP) approached the target level. The horizontal dashed line indicates the target AP level.

Bottom). The time required for the AP response to reach 90% of the target AP decrease was 38±10 s. Thereafter, the error remained very small until the end of the 10-min regulation. The standard deviation of the steady-state error was 1.3±0.1 mmHg. After the end of the feedback regulation, the error signal gradually returned to approximately 20 mmHg.

Figure 6 represents typical results of the supplemental protocols. Electrical stimulation of the triceps surae muscle (denoted as "MS") did not change AP significantly in spite of visible twitching of the stimulated muscle, suggesting that the depressor response to HES was not the outcome of the direct muscle stimulation (**Figure 6A**). Sectioning the ipsilateral sciatic nerve abolished the depressor effect of HES, suggesting that somatic afferent signals were delivered through the sciatic nerve to the central nervous system during HES (**Figure 6B**).

Discussion

We identified the dynamic input–output relationship between HES and the AP response. By using the model transfer function from HES to AP, we were able to develop a servo-controller that automatically adjusted the HES command to reduce AP at a prescribed target level.

Development of the Feedback Controller

The stimulus current-AP response relationship showed a monotonous decreasing slope (**Figure 2C**). Because the effect of the pulse width was statistically insignificant, we chose the stimulus current as a primary control variable. The problem with using the stimulus current for the control variable was that a certain threshold current existed between 0 and 1 mA where the AP response to HES became discontinuous. If the stimulus current happened to be feedback controlled near the threshold current, AP showed significant oscillation around the target level (**Figure 7**, see Appendix B for details). To avoid such a problem related to the threshold current, we set the minimum current to 1 mA (above the threshold current) and used the stimulus frequency as a secondary control variable (**Figure 4B**).

The stimulus frequency-AP response relationship revealed a valley-shaped curve with the nadir of approximately 10 Hz (**Figure 2D**). The result is similar to that obtained by stimulating hamstring muscle afferent nerves[26] From the viewpoint of controller design, the valley-shaped input–output relationship is troublesome because the proportional-integral controller only assumes a monotonous input–output relationship[23] To avoid the problem of the valley-shaped input–output relationship, we limited the stimulus frequency to the range from 0 to 10 Hz (**Figure 4B, Right**). A similar strategy of selecting the monotonous input–output portion was used in a previous study[12]

We quantified the dynamic AP response to HES using a transfer function analysis (**Figure 3B**), and modeled it by a second-order low-pass filter with a pure dead time (**Figure 3C**). Once the transfer function is modeled, we could construct a numerical simulator for the feedback controller design (**Figure 4A**). Because the optimization of control parameters usually requires a number of trials, even if the initial values are selected via classical methods such as the Ziegler–Nichols' method[23] it is impractical to determine optimal parameter values without using the simulator. The simulation results indicated that the integral gain value of 0.005 would provide rapid and stable AP regulation (**Figure 4C**). Because the controller was designed via intensive simulations, AP was actually controlled at the target level with a small variance (**Figure 5B, Bottom**). Note that the current and frequency of HES were automatically adjusted and individualized via the feedback mechanism (**Figure 5A**).

Bionic Strategies Using Neural Interfaces

A framework of treating cardiovascular diseases using neural interfaces is intriguing because the autonomic nervous system exerts powerful influences on the circulatory system. In previous studies, we identified the dynamic characteristics of the arterial baroreflex system and used them to design an artificial vasomotor center. The artificial vasomotor center was able to control AP by stimulating the celiac ganglia in anesthetized rats[10,11] or the spinal cord in anesthetized cats[12] The strength and rapidity of the neural effect on the cardiovascular system compared with that of the

humoral effect[27,28] make the neural interventions desirable for the rapid and stable restoration of AP against acute disturbances such as those induced by postural changes. Gotoh et al demonstrated that a direct neural interface to the rostral ventrolateral medulla also enabled rapid and stable restoration of AP during nitroprusside-induced hypotension in conscious rats.[29] The bionic system to control AP has also been applied in human subjects![13]

Although the aforementioned bionic systems aimed to maintain AP against acute hypotension by increasing sympathetic nerve activity![10–13,29] sympathoinhibition might also be required for the treatment of cardiovascular diseases accompanying sympathetic overactivity. Baroreceptor activation is one of the potential sympathoinhibitory neural modulation?[8,9] In the present study we only demonstrated a framework of short-term AP control by HES. With a development of proper implanting electrodes, however, we might be able to control AP chronically using HES. Although carotid sinus baroreceptor stimulation has a potential to treat drug-resistant hypertension? it could activate peripheral chemoreflex by stimulating carotid bodies. HES might circumvent such unintentional chemoreflex activation. Another clinical implication will be the treatment of chronic heart failure. Although the vagal effect of HES was not evaluated in the present study, acupuncture stimulation might facilitate cardiac vagal activity?[30] Because chronic intermittent vagal nerve stimulation increased the survival of chronic heart failure rats,[7] chronic intermittent HES might be used as an alternative method of direct vagal nerve stimulation for the treatment of chronic heart failure.

Study Limitations

First, we did not identify the mechanism of HES. Because sectioning of the ipsilateral sciatic nerve abolished the AP response to HES (**Figure 6B**), somatic afferent is involved in the effect of HES. In a series of studies, Chao et al and Li et al demonstrated that electroacupuncture activated group III and IV fibers in the median nerves and inhibited sympathetic outflow via activation of μ- and δ-opioid receptors in the rostral ventrolateral medulla?[31,32] Whether a similar mechanism underlies in the rapid-onset and short-lasting effect of HES awaits further studies.

Second, we used pentobarbital anesthesia. Although peripheral neurotransmissions of norepinephrine and acetylcholine can be assessed under the same anesthesia,[28,33] because pentobarbital can suppress many neurotransmitters in the central nervous system,[34] anesthesia might compromise the HES effect. Further studies are required to establish the utility of HES in awake conditions.

Third, we set the proportional gain of the controller at zero to avoid pulsatile changes in the HES command. However, other approaches such as that using a low-passed signal of measured AP as a controlled variable might also be effective to avoid the pulsatile variation in the HES command.

Finally, a development of implanting electrodes is the prerequisite for chronic use of HES. Intramuscular electrodes used in functional electrical stimulation might be used for HES but further refinements are clearly needed regarding the positioning of electrodes including the depth of implantation?[35,36]

In conclusion, we identified the dynamic characteristics of the AP response to acupuncture-like HES and demonstrated that a servo-controlled HES system was able to reduce AP at a prescribed target level. Although further studies are required to identify the mechanism of HES to reduce AP, acupuncture-like HES would be an additional modality to exert a quantitative depressor effect on the cardiovascular system.

Acknowledgments

This study was supported by the following Grants: "Health and Labour Sciences Research Grant for Research on Advanced Medical Technology", "Health and Labour Sciences Research Grant for Research on Medical Devices for Analyzing, Supporting and Substituting the Function of Human Body", "Health and Labour Sciences Research Grant (H18-Iryo-Ippan-023) (H18-Nano-Ippan-003) (H19-Nano-Ippan-009)", from the Ministry of Health, Labour and Welfare of Japan, and the "Industrial Technology Research Grant Program" from New Energy and Industrial Technology Development Organization of Japan.

References

1. Bilgutay AM, Bilgutay IM, Merkel FK, Lillehei CW. Vagal tuning: A new concept in the treatment of supraventricular arrhythmias, angina pectoris, and heart failure. *J Thorac Cardiovasc Surg* 1968; **56:** 71–82.
2. Braunwald E, Epstein SE, Glick G, Wechsler AS, Braunwald NS. Relief of angina pectoris by electrical stimulation of the carotid-sinus nerves. *N Engl J Med* 1967; **277:** 1278–1283.
3. Schwartz SI, Griffith LS, Neistadt A, Hagfors N. Chronic carotid sinus nerve stimulation in the treatment of essential hypertension. *Am J Surg* 1967; **114:** 5–15.
4. Vanoli E, De Ferrari GM, Stramba-Badiale M, Hull SS Jr, Foreman RD, Schwartz PJ. Vagal stimulation and prevention of sudden death in conscious dogs with a healed myocardial infarction. *Circ Res* 1991; **68:** 1471–1481.
5. Yang JL, Chen GY, Kuo CD. Comparison of effect of 5 recumbent positions on autonomic nervous modulation in patients with coronary artery disease. *Circ J* 2008; **72:** 902–908.
6. Baba R, Koketsu M, Nagashima M, Inasaka H, Yoshinaga M, Yokota M. Adolescent obesity adversely affects blood pressure and resting heart rate. *Circ J* 2007; **71:** 722–726.
7. Li M, Zheng C, Sato T, Kawada T, Sugimachi M, Sunagawa K. Vagal nerve stimulation markedly improves long-term survival after chronic heart failure in rats. *Circulation* 2004; **109:** 120–124.
8. Zucker IH, Hackley JF, Cornish KG, Hiser BA, Anderson NR, Kieval R, et al. Chronic baroreceptor activation enhances survival in dogs with pacing-induced heart failure. *Hypertension* 2007; **50:** 904–910.
9. Mohaupt MG, Schmidli J, Luft FC. Management of uncontrollable hypertension with a carotid sinus stimulation device. *Hypertension* 2007; **50:** 825–828.
10. Sato T, Kawada T, Shishido T, Sugimachi M, Alexander J Jr, Sunagawa K. Novel therapeutic strategy against central baroreflex failure: A bionic baroreflex system. *Circulation* 1999; **100:** 299–304.
11. Sato T, Kawada T, Sugimachi M, Sunagawa K. Bionic technology revitalizes native baroreflex function in rats with baroreflex failure. *Circulation* 2002; **106:** 730–734.
12. Yanagiya Y, Sato T, Kawada T, Inagaki M, Tatewaki T, Zheng C, et al. Bionic epidural stimulation restores arterial pressure regulation during orthostasis. *J Appl Physiol* 2004; **97:** 984–990.
13. Yamasaki F, Ushida T, Yokoyama T, Ando M, Yamashita K, Sato T. Artificial baroreflex: Clinical application of a bionic baroreflex system. *Circulation* 2006; **113:** 634–639.
14. Li P, Pitsillides KF, Rendig SV, Pan HL, Longhurst JC. Reversal of reflex-induced myocardial ischemia by median nerve stimulation: A feline model of electroacupuncture. *Circulation* 1998; **97:** 1186–1194.
15. Longhurst JC. Electroacupuncture treatment of arrhythmias in myocardial ischemia. *Am J Physiol Heart Circ Physiol* 2007; **292:** H2032–H2034.
16. Lujan HL, Kramer VJ, DiCarlo SE. Electroacupuncture decreases the susceptibility to ventricular tachycardia in conscious rats by reducing cardiac metabolic demand. *Am J Physiol Heart Circ Physiol* 2007; **292:** H2550–H2555.
17. Ohsawa H, Okada K, Nishijo K, Sato Y. Neural mechanism of depressor responses of arterial pressure elicited by acupuncture-like stimulation to a hindlimb in anesthetized rats. *J Auton Nerv Syst* 1995; **51:** 27–35.
18. Uchida S, Shimura M, Ohsawa H, Suzuki A. Neural mechanism of bradycardiac responses elicited by acupuncture-like stimulation to a hind limb in anesthetized rats. *J Physiol Sci* 2007; **57:** 377–382.
19. Michikami D, Kamiya A, Kawada T, Inagaki M, Shishido T, Yamamoto K, et al. Short-term electroacupuncture at Zusanli resets the arterial baroreflex neural arc toward lower sympathetic nerve

activity. *Am J Physiol Heart Circ Physiol* 2006; **291:** H318–H326.
20. Yamamoto H, Kawada T, Kamiya A, Kita T, Sugimachi M. Electroacupuncture changes the relationship between cardiac and renal sympathetic nerve activities in anesthetized cats. *Auton Neurosci: Basic and Clinical* 2008; **144:** 43–49.
21. Marmarelis PZ, Marmarelis VZ. Analysis of Physiological Systems. The white noise method in system identification. New York: Plenum; 1978.
22. Snedecor GW, Cochran WG. Statistical Methods, 8th ed. Ames, Iowa: University Press; 1989.
23. Åström K, Hägglund T. PID Controllers: Theory, Design, and Tuning, 2nd ed. City of Publication: Instrument Society of America; 1995.
24. Kawada T, Sunagawa G, Takaki H, Shishido T, Miyano H, Miyashita H, et al. Development of a servo-controller of heart rate using a treadmill. *Jpn Circ J* 1999; **63:** 945–950.
25. Kawada T, Ikeda Y, Takaki H, Sugimachi M, Kawaguchi O, Shishido T, et al. Development of a servo-controller of heart rate using a cycle ergometer. *Heart Vessels* 1999; **14:** 177–184.
26. Johansson B. Circulatory responses to stimulation of somatic afferents with special reference to depressor effects from muscle nerves. *Acta Physiol Scand* 1962; **Suppl 198:** 1–91.
27. Kawada T, Miyamoto T, Miyoshi Y, Yamaguchi S, Tanabe Y, Kamiya A, et al. Sympathetic neural regulation of heart rate is robust against high plasma catecholamines. *J Physiol Sci* 2006; **56:** 235–245.
28. Kawada T, Yamazaki T, Akiyama T, Shishido T, Miyano H, Sato T, et al. Interstitial norepinephrine level by cardiac microdialysis correlates with ventricular contractility. *Am J Physiol Heart Circ Physiol* 1997; **273:** H1107–H1112.
29. Gotoh TM, Tanaka K, Morita H. Controlling arterial blood pressure using a computer-brain interface. *Neuroreport* 2005; **16:** 343–347.
30. Nishijo K, Mori H, Yosikawa K, Yazawa K. Decreased heart rate by acupuncture stimulation in humans via facilitation of cardiac vagal activity and suppression of cardiac sympathetic nerve. *Neurosci Lett* 1997; **227:** 165–168.
31. Chao DM, Shen LL, Tjen-A-Looi S, Pitsillides KF, Li P, Longhurst JC. Naloxone reverses inhibitory effect of electroacupuncture on sympathetic cardiovascular reflex responses. *Am J Physiol Heart Circ Physiol* 1999; **276:** H2127–H2134.
32. Li P, Tjen-A-Looi SC, Longhurst JC. Rostral ventrolateral medullary opioid receptor subtypes in the inhibitory effect of electroacupuncture on reflex autonomic response in cats. *Auton Neurosci: Basic and Clinical* 2001; **89:** 38–47.
33. Kawada T, Yamazaki T, Akiyama T, Li M, Ariumi H, Mori H, et al. Vagal stimulation suppresses ischemia-induced myocardial interstitial norepinephrine release. *Life Sci* 2006; **78:** 882–887.
34. Adachi YU, Yamada S, Satomoto M, Watanabe K, Higuchi H, Kazama T, et al. Pentobarbital inhibits L-DOPA-induced dopamine increases in the rat striatum: An in vivo microdialysis study. *Brain Res Bull* 2006; **69:** 593–596.
35. Guevremont L, Norton JA, Mushahwar VK. Physiologically based controller for generating overground locomotion using functional electrical stimulation. *J Neurophysiol* 2007; **97:** 2499–2510.
36. Hardin E, Kobetic R, Murray L, Corado-Ahmed M, Pinault G, Sakai J, et al. Walking after incomplete spinal cord injury using an implanted FES system: A case report. *J Rehabil Res Dev* 2007; **44:** 333–346.

Appendix A

Framework of the Feedback Controller

Figure 4A is a simplified block diagram of the feedback controller system used in the present study. The controller was based on a proportional-integral controller[23–25] $G(f)$ represents the transfer function of the controller.

$$G(f)=-K_P+\frac{-K_I}{2\pi fj} \quad \text{(A1)}$$

where K_P and K_I denote proportional and integral gains, respectively. j represents the imaginary unit. Negative signs for the proportional and integral gains compensate for the negative input–output relationship between HES and the AP response. $H(f)$ represents a model transfer function from HES to AP determined from Protocol 3. The measured AP can be expressed as:

$$AP_{Measured}(f)=H(f)HES(f)+AP_{Noise}(f) \quad \text{(A2)}$$

where $AP_{Noise}(f)$ is the AP fluctuation such as that associated with changes in animal conditions. The controller compares the measured AP with the target AP, and adjusts the HES command to minimize the difference between them according to the following equation:

$$HES(f)=G(f)[AP_{Target}(f)-AP_{Measured}(f)] \quad \text{(A3)}$$

By eliminating $HES(f)$ from the equations A2 and A3, the overall controller characteristics are described as:

$$AP_{Measured}(f)=\frac{G(f)H(f)}{1+G(f)H(f)}AP_{Target}(f)+\frac{1}{1+G(f)H(f)}AP_{Noise}(f) \quad \text{(A4)}$$

The equation A4 indicates that if $G(f)$ is properly selected so that $G(f)H(f)$ becomes by far greater than unity, the measured AP approaches the target AP whereas the noise term is significantly attenuated over the frequency range of interest.

Appendix B

Problem with the Threshold Current

We tried to adjust the intensity of HES by the stimulus current alone. When the stimulus current happened to be feedback controlled near a threshold current, however, the controller showed an on–off type controller behavior around the target AP level, as shown in **Figure 7**. At time zero, the controller was activated. The stimulus current increased to approximately 2.7 mA in the beginning and then decreased to a value below 1 mA, accompanying the AP reduction around a target level (a horizontal dashed line). However, the stimulus current and AP did not stabilize. Because the AP response was discontinuous at the threshold current (ie, the depressor effect of HES was abruptly turned on and off), the controller could not adjust the stimulus current in a continuous manner. To avoid this kind of on–off type controller behavior, we introduced the stimulus frequency as the secondary control variable (**Figure 4B**).